A PROPOSAL TO INVESTIGATE THE FORMATION OF CHARMONIUM STATES USING THE PBAR ACCUMULATOR RING

V.Bharadwaj, J.Griffin, S.Holmes, W.Kells, J.MacCarthy

J.MacLachlan, J.Peoples, P.Rapidis, D.Young

Fermi National Accelerator Laboratory

R.Calabrese, P.Dalpiaz, P.Ferretti-Dalpiaz, E.Lupi,

F.Petrucci, M.Saurie

Universita' di Ferrara

M. Mainelli, M.Mattera, F.Tommassini, V.Valbusa

Universita' Di Genova

G.Borreani, R.Cester, E.Menichetti, S.Palestini, N.Pastrone,

G.Rinaudo, L.Tecchio

Universita' di Torino

Spokesperson : R.Cester

Local contact : P.Rapidis

March 1985

1. Introduction

The exclusive formation of bound $\bar{c}c$ states in $p\bar{p}$ collisions was observed in a recent experiment[1] (R704) at the CERN ISR, thereby demonstrating the feasibility of using the $p\bar{p}$ reaction as a means of measuring the mass and width of states of charmonium which are not directly accessible to electron-positron colliders. The success of the experiment was due to the use of a novel method for obtaining a high luminosity antiproton annihilation source with excellent definition of the initial state energy. This was accomplished by letting a continuously transversely and longitudinally cooled antiproton beam, stored in ring 2 of the ISR, interact with a high density H_2 gas jet target crossing the ISR vacuum pipe. This setup featured both a very small interaction volume and a beam with good momentum definition and small transverse emittance, even after many hours of operation.

We propose to study the properties of charmonium states in a $p\bar{p}$ formation experiment in the Fermilab Accumulator Ring using the same method that some of us used at the ISR. The Fermilab Accumulator Ring and its associated cooling systems will make it possible to do a vastly superior experiment than the exploratory experiment done at the ISR. The reasons for the improvement are:

1. The stored antiproton current will be a factor of five greater than was typically achieved at the ISR. In addition, the accumulation rate of antiprotons will be $\sim 10^{11}$ antiprotons/hour vs. $\sim 10^{11}$ antiprotons in 12 hours. These differences will lead to a significantly higher integrated luminosity.

2. The Antiproton Source stochastic cooling systems, as currently

implemented, will constrain the energy spread (FWHM) of the beam to $\Delta E/E \sim 2 \times 10^{-4}$, corresponding to a mass resolution of 300 KeV/c^2(FWHM) at 3 GeV/c^2.

3. The large acceptance detector which we describe will incorporate the features that have been found to be essential in the discrimination of the signal over the background at the R704 experiment.

4. The detector acceptance will be roughly 5 times larger than that of R704. When this is considered together with the fact that sufficient running time should be available at the Accumulator, in contrast to the situation created by the closing of the ISR, it is seen that the experiment will not be statistics limited.

We note that the scheduling of the experiment should not present any difficulty, since we propose to run it during periods of fixed target operation of the Tevatron. We have assumed that the Main Ring can operate in the same manner as it is operating during Antiproton Source commissioning. This method of operation has not affected the fixed target operation.

2. Physics Objectives

Ten years after the discovery of the ψ the experimental information on charmonium states is still quite incomplete. The mass spectrum (Fig. 1) of $\bar{c}c$ states, as predicted by a non-relativistic potential model, has not been fully verified. Although the 2^1S_0 state (η_c') has been seen in one experiment[2], compelling evidence is desirable. The first orbital excitation of the singlet state, the $^1P_1$, has not been established. A statistically weak indication that it might be at the center of gravity of the ^3P states was obtained from the measurement of inclusive ψ production in $p\bar{p}$ interactions[3]. The $^1D_2$ and $^3D_2$ states, which may be narrow, have never been detected. Moreover, even for those states which have been convincingly established, such as the $^1S_0$ and the ^3P's, a precise determination of their mass, total width, partial width to electromagnetic channels and branching ratios to hadronic channels is still lacking.

Indeed, the only states for which these parameters have been accurately measured are those which have the quantum numbers of the γ, ($J^{PC}=1^{--}$). This is a consequence of the fact that these are the only states which can be directly formed in e^+e^- colliders through the first order QED process: $e^+e^- \rightarrow \gamma \rightarrow \bar{c}c \rightarrow$final states.

The study of these fundamental parameters of charmonium states with quantum numbers different from 1^{--} is at best a difficult task at e^+e^- colliders. The ^1S and ^3P states are produced in the radiative decay of ψ' and ψ. Because the precision in the measurement of mass and total width is limited by the energy resolution of the detector, it is not possible to determine the total widths and masses of these states with the same precision as the measurements of the ψ and ψ'.

This difficulty can be avoided when the $\bar{c}c$ states are formed in exclusive $p\bar{p}$ annihilations. Since all $c\bar{c}$ states can be directly formed in $p\bar{p}$ annihilation, the

determination of the resonance parameters (mass and total width) can be performed by measuring the yield of the state of interest as a function of energy of the initial state. Provided a good signature is available for detecting the final state of interest, this determination is limited only by the characteristics of the beam and target system. The properties of the Accumulator and the gas jet make it possible to determine the mass to great accuracy, perhaps to the same accuracy as for the ψ determination, and the total width to an accuracy of better than 300 KeV/c^2.

The main difficulty which must be overcome in a $p\bar{p}$ annihilation experiment, is the extraction of the small signal out of a very large non-resonant hadronic background. This can be done by detecting the electromagnetic decays of the resonant states. Our proposed detector is designed to detect these states efficiently, while rejecting the hadronic background. We have also considered the possibility of detecting charmonium states through their decay into OZI forbidden hadronic channels (for example: $^1S_0 \rightarrow \phi\phi \rightarrow 2K^+2K^-$) and we have made the detector sensitive to these states.

To illustrate the advantages of a $p\bar{p}$ experiment we show in Figure 2a a comparison of the Crystal Ball data for all fully reconstructed χ events from the reaction:

$$e^+e^- \rightarrow \psi' \rightarrow \chi_{1,2} + \gamma \rightarrow \psi + \gamma + \gamma \rightarrow e^+e^- + \gamma + \gamma$$

and the R704 data for:

$$p\bar{p} \rightarrow \chi_{1,2} \rightarrow e^+e^- + \gamma$$

In Figure 2b we show the same comparison with the anticipated results from the experiment we hope to do at Fermilab for data taken over an equivalent running period to the R704 run (3 weeks).

We propose to study the following channels (in order of increasing resonance mass):

1) $p\bar{p} \to \eta_c \to \gamma\gamma$
$\quad\quad\quad\quad \to \phi\phi \to 2K^+\ 2K^-$

2) $p\bar{p} \to \chi_0 \to \psi+\gamma \to e^+e^-+\gamma$
$\quad\quad\quad\quad \to \gamma\gamma$

3) $p\bar{p} \to {}^1P_1 \to \psi+\pi^0 \to e^+e^-+\pi^0$ (Isopin violating)
$\quad\quad\quad\quad \to \psi+\pi^++\pi^- \to e^+e^-+\pi^++\pi^-$
$\quad\quad\quad\quad \to \eta_c+\gamma \to \gamma\gamma+\gamma$
$\quad\quad\quad\quad \to \eta_c+\gamma \to \phi\phi+\gamma$

4) $p\bar{p} \to \chi_{1,2} \to \psi+\gamma \to e^+e^-+\gamma$

5) $p\bar{p} \to \eta_c' \to \gamma\gamma$
$\quad\quad\quad\quad \to \phi\phi \to 2K^++2K^-$

6) $p\bar{p} \to {}^1D_2 \to \gamma\gamma$
$\quad\quad\quad\quad \to \phi\phi \to 2K^++2K^-$
$\quad\quad\quad\quad \to \psi+\pi^++\pi^-+\pi^0 \to e^+e^-+\pi^++\pi^-+\pi^0$

7) $p\bar{p} \to {}^3D_2 \to \chi\gamma \to \psi+\gamma\gamma \to e^+e^-+\gamma\gamma$
$\quad\quad\quad\quad \to \psi+\pi^++\pi^0+\pi^- \to e^+e^-+\pi^++\pi^{0+}+\pi^-$

In each case the systematic errors on mass and total width measurements are expected to be <100 KeV.

From 1) and 2) a measurement of BR(Resonance $\to \gamma\gamma$) will be obtained.

A comprehensive set of theoretical predictions which relate the measured parameters has been obtained within the framework of perturbative QCD[4]. The comparison with precise experimental results will establish the degree to which perturbative QCD works in the Q^2 region around 10 GeV^2.

From 2) and 4) we can measure the BR(Resonance $\to p\bar{p}$).

From the point of view of perturbative QCD this is also an interesting result

since a whole formalism has been developed to handle exclusive processes of the type $p\bar{p}\to$heavy meson resonance[5].

The R704 data show an accumulation of ψ inclusive events close to the center of gravity of the ^3P states. It is important to prove that this signal is related to $^1P_1$ formation and to measure precisely the mass splitting ΔM=mass($^1P_1$)-energy($^3P_{c\ of\ g}$) which arises from spin-spin forces. If the spin dependent force, which involves the color magnetic field, is short-range, one indeed expects ΔM to be small[6].

The two states $^1D_2$ and $^3D_2$ are predicted in potential models at about 3.815 GeV, slightly below the $D\bar{D}^*(D^*\bar{D})$ threshold. Since their decay to $D\bar{D}$ is forbidden by parity conservation, they are expected to be narrow. Their discovery and the precise measurement of the mass splitting between the $^3D_2$ and the $^3D_1$ states and between $^3D_2$ and $^1D_2$, would shed light onto the structure of spin-orbit forces[7].

Other interesting pieces of information can also be extracted from the data. For example, a significant sample of χ_2 events will allow a precise measurement of the angular distributions of the decay products with a good sensitivity to the multipole contributions in the $\chi\to\psi+\gamma$ decay and to the relative admixture of the $\lambda=\lambda_{\bar{p}} - \lambda_p=0,1$ helicity states of the resonant $p\bar{p}$ system. A systematic background study, off-resonance, triggering on inclusive high-mass e^+e^- final states will allow limits to be set on the process $p\bar{p}\to e^+e^-$ which measures the proton form factor, in the high Q^2 time-like region, and provide a measurement of the cross section of the continuum process $p\bar{p}\to\psi\pi^0$ which is sensitive to the relative admixture of $L=J\pm1$ in the wave function of the resonating $p\bar{p}$ system[8]. Finally, it will provide a method for exploring the mass region below open charm, for exotic states with some charm content.

3. Detector Requirements

a) Design goals and guidelines:

The efficient detection of electromagnetic final states from charmonium decay provides a powerful tool for the accurate measurement of the fundamental parameters of the $c\bar{c}$ system, as well as a sensitive probe for finding the missing states. On the other hand, the small value of the cross sections for producing the final states require a large acceptance detector. The high level of hadronic background demands that the detector possess accurate tracking for both charged particles and gamma rays, good energy resolution for electrons and gammas, and finally very good e/h discrimination. It should be mentioned that π^0/γ separation, a crucial requirement for many of the physics topics we want to investigate, can only be achieved by designing a detector which has excellent spatial resolution for two-shower identification, and good detection efficiency for gammas with energies as low as 50 MeV. A further requirement is the ability to handle an interaction rate as large as 1.0 MHz, since the luminosity will be limited by this feature of the detector rather than the antiproton beam current or the gas jet target density. This last requirement rules out long drift paths and slow scintillators, and also points to the need for some redundancy, particularly in the tracking chambers.

The need for a large acceptance makes it difficult to design a magnetic spectrometer that will fit in the severely confined space of the Antiproton Source Enclosure. On the other hand, by concentrating on e/γ final states one is naturally lead into choosing a non-magnetic, high granularity calorimeter for the detector. Such a device was successfully operated in the R704 experiment at the CERN ISR[1]. It should be stressed that the quasi-pointlike interaction area inherent to the jet-target/pbar beam complex greatly facilitates the design,

leading in a natural way to a compact geometry.

b) Acceptance

By covering polar angles between 15 and 70 degrees and the full azimuth an acceptance of ≥50% for e^+e^-, $\gamma\gamma$ and $e^+e^-\gamma$ final states is obtained. The natural detector geometry for this fixed target experiment is cylindrical, with its axis lying along the beam line. This cylindrical symmetry is closely reflected in each detector element, with the exception of the forward endcap.

c) Tracking

Tracking will be provided by a central, multi-layer, cylindrical mini-drift chamber, with 9 independent θ and φ measurements. Drift time will measure ϕ angles, and charge division will be used to measure θ. A transverse track resolution of 250 micrometers from the measurement of drift times and 1% longitudinal position measurement from charge division will lead to errors of about 3 mrad in θ and 1.5 mrad in ϕ. The angular resolution in θ is achieved by a careful design of the longitudinal profile of the chamber, whose sensitive length gradually increases from the inner to the outer layers, resulting in an optimal match of acceptance and resolution requirements. In the forward endcap, a standard planar MWPC will provide good position measurement down to $\theta = 7°$.

d) Electron tagging

A threshold gas Cerenkov counter will be used to tag electrons. When filled with Freon-13 at atmospheric pressure, such a counter (with the geometry and optical system described below) will yield ≥5 photoelectrons per electron track. The pion rejection ratio is about 0.001 up to 3.7 GeV/c[9]. The light yield is sufficient to ensure good electron efficiency, and to some extent it will make it possible to reject e^+e^- pairs from early γ conversion which have unresolved opening angles.

e) Calorimetry

The electromagnetic calorimeter will posses good energy resolution up to 5-6 GeV, good spatial resolution and two-shower separation, and high detection efficiency for low energy γ's. The reasons for these requirements are as follows:

i) Good energy resolution is needed to single out the e^+e^- signal from ψ decay. This channel represents one of the major ways of identifying the presence of charmonium in the final state. It is also essential in identifying 2γ final states.

ii) While a good spatial resolution is needed for ψ detection as well as for reconstructing the mass of charmonium states decaying into $\gamma\gamma$, such a good resolution is even more important in being able to separate two nearby showers from symmetric π° decays. This is essential in rejecting the large π° background.

iii) Good detection efficiency of low energy γ's, down to about 30 MeV is needed in order to distinguish asymmetric decays of π°'s from a single γ. This is a crucial requirement for the whole experiment, and leads one to choose special solutions for the first 3 to 4 radiation lengths of the calorimeter.

Longitudinal segmentation should also be implemented in order to improve the e/h discrimination provided by the Cerenkov counter and the total energy measurement.

4. Estimation of Cross Sections and Luminosity Requirements

We shall concentrate first on the η_c, χ_1, χ_2, and the $^1P_1$ states that have already been explored in R704. The available information on cross sections and backgrounds is reported in Table I together with a projection for the proposed experiment. For comparison we include also the same information on the ψ since it was used for the energy calibration in R704 and could be used in this experiment for the same purpose. The effective cross sections for R704 given in the table are based on the number of reconstructed events and are defined as follows: number of events/sec = $\sigma^{eff} * L_o$, where L_o is the instantaneous luminosity. The projected values for this experiment are obtained from the R704 results by scaling by the relative geometrical acceptance ratio of the proposed detector to the R704 detector. The background estimates are therefore upper limits. In the ensuing discussion we will point out the drastic improvements we expect over the R704 performance which arise from the improved detector design of this proposal.

R704 had a geometrical acceptance ranging from 9% to 12% depending on the specific channel. The acceptance of the proposed detector will be a factor 4 to 5 times larger. The C.M. energy resolution will be improved by a factor of 4. Since one of the main goals of the experiment is the measurement of the excitation profiles of the resonances, this improved resolution is of great value. We have made Monte Carlo simulations of resonance production with negligible background and a total width larger than the C.M. energy resolution and we find that a reasonable scanning procedure is to subdivide the available luminosity between 5 energy settings spanning the resonance width and separated by half a total width. This will lead to an average rate of $(.2+.5+1+.5+.2)/5 = 0.48$ times the peak rate, obtained when the beam energy is centered on the resonsance. Our estimates of the number of events take this approximate factor of 2 into account.

We now illustrate through various examples the capabilities of the proposed experiment.

$\chi_1 \to \psi + \gamma$.

From a scan with an integrated luminosity of 5000 nb^{-1} around the resonance we expect ~1600 events of the type $\chi_1 \to e+ e- + \gamma$. Monte Carlo simulations and projections from the R704 results indicate that the expected precision in the measurements of the total width of the χ_1 and of the branching ratio into $p\bar{p}$ will be 6% to 12% for a total width in the range of 1 MeV to 0.1 MeV, respectively.

$\chi_2 \to \psi + \gamma$.

From a similar scan with 5000 nb^{-1} luminosity we anticipate collecting ~2000 events of the type $\chi_2 \to e^+e^- + \gamma$, which will allow us to measure the total width and the branching ratio to $p\bar{p}$ with a statistical error of 6%.

$\chi_2 \to \gamma + \gamma$

As a by-product of the χ_1 and χ_2 measurements we will search for the decay $\chi_2 \to \gamma + \gamma$. The forbidden process $\chi_1 \to \gamma + \gamma$ will enable us to estimate the non resonant $2\pi^\circ$ background at the χ_2. For a background rejection similar to that of R704 we estimate a signal of 115 ±24 events above a background of 225 events (signal=σ(peak)/2=23 pb ; background=45 pb). Should the background be found to be smaller (e.g. signal=σ(peak)=46 pb, background=25 pb) a subsequent dedicated run of 5000 nb^{-1} at the peak of the χ_2 resonance could yield a signal of 230 events over a background of 125 events, thus allowing a measurement of BR($\chi_2 \to \gamma + \gamma$) with 10% precision. This additional run will also provide ~4000 $\chi_2 \to \psi + \gamma$ events useful for the study of the mechanism of that decay.

$\eta_c \rightarrow \gamma + \gamma$

Here the first goal is to clearly observe the $\gamma+\gamma$ decay mode. For an integrated luminosity of 2500 nb^{-1} on the resonance and an equivalent luminosity off the resonance, and an η_c cross section times branching ratio into 2 γ's of 50 pb, we expect a signal of 125 ±22 events above a background of 175 events (background= 70 pb). Should such a run establish an observable signal, a subsequent scan around the resonance with a total integrated luminosity of 10 000 nb^{-1} will yield a measurement of the total width of the η_c and of $BR(\eta_c \rightarrow \gamma\gamma)$. On the basis of a Monte Carlo calculation we anticipate a precision for these measurements of 20% and 15% respectively.

$^1P_1 \rightarrow \psi + \ldots$

The expected background for the proposed experiment, based on R704 results, is 40 pb. Since the detector proposed for this experiment features fine-grained tracking of charged and neutral particles over the full acceptance, there will be a major qualitative improvement in the background suppression. This will occur because we will be able to fully reconstruct, with good detection efficiency, the final states $\psi + \pi+ \pi- \rightarrow e^+e^- + \pi+ \pi-$ and $\psi + \pi^\circ \rightarrow e^+e^- + \gamma + \gamma$. These states should represent a large fraction of the $\psi \rightarrow e^+e^-$ inclusive sample.

An exploratory run with an integrated luminosity of 5000 nb^{-1} at energies equally divided between the center of gravity of the χ states (3526 MeV) and at energies 5 MeV above and below the χ_c of g energy, should establish whether the small cluster of ψ inclusive events observed by R704 is significant. The background will be measured with a sensitivity 30 times higher than the one in R704. We expect 40 to 140 events from such a run. Even though a firm prediction

is impossible, it is quite likely that such a run will lead to a discovery, if the background is 10 times less than the upper limit set by R704.

5. Antiproton Source

In this section we describe the requirements this experiment places on the Antiproton Source.

We have assumed a luminosity $10^{31}/cm^2sec$ in preparing our event estimates. We do not plan to aim for a higher luminosity since this luminosity leads to a 1 MHz instantaneous rate summed over all detector elements (σ(tot) = 70 mb). This luminosity can be achieved with 1.5×10^{11} circulating antiprotons, a jet density of ~ 1.2×10^{14} atoms/cm^3, and a jet thickness ~ 0.9 cm. The jet density is chosen to be 0.8 of the maximum achieved in R704 in order to guarantee beam lifetimes in excess of 24 hours, limited disturbance to the vacuum system, and limited pumping requirements. We consider, for example, the operation scheme of one pbar fill per day and 20 hours of data taking. With 90% data taking efficiency, we would collect each day 600 events/nb. Measurements such as those of the χ widths, and for the exploratory runs used to measure the 2γ decays of the η_c and $^1P_1$ states would each take 10 days. The measurement of the η_c width would require 20 days of data taking.

A scenario for the operation of the Antiproton Source that will lead to a stored beam of 1.5×10^{11} antiprotons, with energy of 3 to 6.5 GeV, transverse emittance of 2π mm-mrad, and momentum spread of $\pm .5$ MeV, is described in the Appendix. It can be seen that such an operation is well within the capabilities of the Source.

The proposed location for this experiment is the middle of the low dispersion straight section in A-50. The severe space constraint that the small size of the Antiproton Source Enclosure imposes can be aleviated if one excavates a small pit in the floor of the tunnel. A reasonable size detector, as the one we propose, can be accomodated if a pit 24" deep, 60" wide, and 80" long is constructed.

6. Gas Jet Target

The target system is based on the technique of molecular cluster jet beams. In the isoentropic expansion of a gas from high pressure and low temperature through a nozzle of special geometry and very small throat a flux of agglomerates of very large numbers of molecules is created. These clusters are flying in the direction of the expansion axis at supersonic speeds (fig.3). The structure of the target system will be the same as the one used in the R704 experiment[1].

The expansion chamber is separated from the Accumulator vacuum pipe by two differential pumping stages in order to make compatible the pressure conditions in the expansion chamber and in the accumulator vacuum chamber. The H_2 beam is absorbed, after having traversed the accumulator vacuum pipe, by a powerful pumping system which is separated from the vacuum pipe of the accumulator by a differential pumping stage, again in order to make compatible the pressures.

A system of collimators will define the dimensions of the H_2 beam at the crossing with the antiproton beam. The initial conditions of the H_2 before the expansion are : P = 10 bar T = 77°K. The expansion nozzle will be 'trumpet-shaped' [1] with a throat diameter of 30 microns. A surface density of 10^{14} atoms/cm^2 was obtained in R704 at the region of overlap of the jet with the antiproton beam. The pumping systems will be consist of turbomolecular pumps (expansion chamber and 1 differential pumping stage), and Non Evaporable Getters (main pump for absorption and the other differential pumping stages).

A special system of pumps acting on the accumulator vacuum pipe will reduce the pressure in the interaction region in such a way that the gas diffusing around the H_2 beam (H_2 which diffuses from the production system and backstreaming from the absorption system) will only be 1-2% of the gas flying in the jet. Two fast

ultra high vacuum valves will separate the production and absorption stages from the accumulator vacuum pipe. In this way when not in use the target system will be completely isolated from the accumulator vacuum pipe.

7. Detector Design

a. Design goals and guidelines

The requirements for a detector were enumerated in section 3. They include accurate tracking, good electron/hadron separation, good π^0-γ separation, good detection efficiency for low energy photons (down to ~50 MeV), large acceptance and high rate capability (up to 1 MHz).

A detector which meets these general requirements must also meet the severe space restrictions imposed by the Antiproton Source Enclosure. This restriction rules out the general class of magnetic spectrometers, since the detector must be contained in a cyclinder centered on the beam axis with a radius of no more than 120 cm. A high granularity non-magnetic detector which meets both the aforementioned general requirements and the space constraints of the tunnel can be made to be an excellent large acceptance detector of electrons and photons. For that reason we have chosen to use a high granularity electromagnetic calorimeter as the major element in the proposed detector. In order to be able to further discriminate electrons from hadrons we have incorporated a track chamber and a Cerenkov counter into the detector. An overall view of the detector is shown in Fig. 4.

b. Tracking

To ensure good accuracy in θ and ϕ measurements, we have designed a central tracking device, which should be able to handle the high interaction rate from the high luminosity annihilation source. A general sketch of this device is shown in Figs. 5 and 6. Nine layers of sense wires will be used to measure radial and ϕ coordinates using drift times, while charge division will provide z measurement (i. e. θ measurement). The maximum drift time is kept at about 100 ns, allowing

for handling of relatively high event rates. The drift chamber gas gain will be set rather low (10^3 to 10^4) in order to obtain good chamber efficiency and lifetime. This last feature will require the use of fast, low noise front-end electronics for the charge division read-out. By using different chamber lengths in the various regions of polar angle θ, good z-resolution can be obtained over the whole acceptance. With nine sensitive layers, assuming a conservative resolution of 250 microns from drift length and 1%*length from charge division, one should obtain angular resolution of about 3 mrad in θ and 1.5 mrad in ϕ.

We plan to install 3 small cylindrical MWPC's inside the innermost cathode layer of the drift chamber, with 2 mm pitch and 3-4 degrees of stereo tilt on two of them. These will both improve the offline pattern recognition and will be very helpful in the construction of a refined, high level trigger. A summary of the 12 sensitive layers of the central detector is contained in Table II. We are now starting a detailed feasibility study of the mechanical construction of this chamber, as well as tests of the charge division resolution on short wires, and of the overall chamber response at high rates.

b. The Cerenkov Counter

In the energy range of the experiment, it is possible to tag electrons with a threshold gas Cerenkov counter operated at atmospheric pressure. The fast signals from this counter can be used in the first level trigger. We have designed a counter where the Cerenkov radiator occupies a cylindrical volume inside the calorimeter walls (Fig. 7) leaving the space close to the interaction point open for the tracking detector. The design of the optical system is greatly simplified by the fact that the small interaction volume is a point source of particles. The object size is defined by the Cerenkov light cone aperture. In our design the focusing mirror is an ellipsoid of revolution tangential to the R=60 cm cylinder,

with major semiaxis along the beam (100 cm long) and the minor semiaxis equal to 60 cm, with one focus placed at the interaction point. The light from a source at the interaction point (A) is focused to the other focus (B), on the beam axis, 160 cm downstream of the source.

A system of 6 small plane mirrors arranged in a pyramidal structure upstream of B deflects the image from the axis on a ring around the beam pipe. By adjusting the pyramid parameters (apex position and angle of the mirrors to the beam) we can optimize the location of the image. With a half-aperture angle of 9 degrees and the apex 33 cm downstream of B, the image is centered on a circle of radius R=10 cm around the beam line. The image half height is 5 to 5.5 cm, so that a large fraction of the light can be collected on a tightly packed double ring of 2" photomultipliers.

The angular region occupied by this system of photomultipliers, as viewed from the target, is 0 to 6 degrees and a small scintillator counter upstream of the pyramidal mirrors, will veto spurious tags due to Cerenkov light produced in the P.M. window by charged particles from the interaction region. Unfortunately this will not remove spurious tags related to photon conversions in the P.M. windows, but these will be infrequent (typical window thickness is 0.015 radiation lengths) and can probably be removed by discriminating on the pulse height.

The radiator length varies from 39 cm at the largest angles (70 degrees) to 100 cm at the smallest ones (15 degrees). We have used a ray tracing computer program to study the geometrical light collection efficiency. With Freon-13 as a radiator gas (θ_{cer}=2.17 degrees) the light collection efficiency is $>\sim$ 85%.

The choice of the gas is dictated as a compromise between two opposite requirements:

a) the index of refraction should be sufficently low to suppress, by the

Cerenkov effect threshold, the hadronic component: $n < 1/\beta_{max}$, with β_{max} the maximum pion velocity, allowed by two body kinematics , within the counter acceptance

b) the index of refraction should be as high as possible to maximize the light yield for $\beta=1$ particles.

As an illustration, if we use Freon 13 with $(n-1)\times10^6=720$ the estimated number of photoelectrons will vary with path length in the radiator from 5 to 12 as the electron production angle (and hence the path length) varies over the range of acceptance ($15° < \theta < 70°$) of the Cerenkov counter.

At $\sqrt{s}$ = 3.1 GeV, pions emitted at $\theta > 20°$ are below threshold. In the angular range between 15° and 20° pions from a 2 body final state are above threshold but can be separated from electrons by discriminating on the light yield (less than 3 photoelectrons for pions vs 12 photoelectrons for $\beta=1$ particles). The situation worsens slightly at the higher center of mass energies but it is still manageable.

The estimate of the number of photoelectrons is obtained by scaling the performance of the counter built for R704, which also operated with Freon-13. When tested using a pion/electron beam, with electron identification, the counter gave a rejection factor of 1000 for pions below threshold[11]. Moreover, the residual signal was explained by delta rays from the pions in the radiator.

Should the construction of the ellipsoidal mirror pose problems, we have designed an alternative Cerenkov counter scheme based on the use of a multicell system with centered spherical optics (Fig.8). A nice feature of this second design is that the four volumes, corresponding to different polar angle intervals, could in principle have independent gas systems. This would permit the use of a gas with lower index of refraction at the smallest angles, where the radiator length is largest. With CO_2, $(n-1)*10^6 = 420$, the average number of photoelectrons (6 to 7) in the angular range between 15 and 26 degrees is still high enough to

ensure very good detection efficiency for $\beta=1$ particles, while pions are always below threshold and are optimally rejected.

c. The calorimeter.

We have considered several alternatives in the design of the calorimeter. One is based on the choice of components, such as BaF_2 crystals and dense scintillating glass, which are only now becoming commercially available in large quantities. A calorimeter using BaF_2 provides significant advantages because its density allows it to be fit into the available space more readily and its energy resolution will be superior to a lead glass calorimeter. In spite of these advantages, the cost of BaF_2 is not now within the range of affordability. Nevertheless the price could decrease as these crystals come into wider use. Since we recognize that it is important to establish that we can design, within an affordable budget, a calorimeter which reaches the stated physics goals, we present a model design using lead glass. This design satisfies the requirements enumerated in section 3 and can be built from readily available components at at a reasonable price. We wish to stress the fact that we are still actively exploring alternative calorimeter designs.

Since this model design draws heavily on the experience obtained from the R704 detector, its calculated performance should be a reliable predictor of actual performance.

Two views of the calorimeter lay-out are given in figs. 4 and 9. The cylndrical shell extending in acceptance from a polar angle of 22 degrees to a polar angle of 75 degrees is completed by an end-cap (fig.10) which covers the forward hemisphere down to 9 degrees.

The longitudinal structure is sketched in fig. 11 and basically consists of two elements: a) 4.5 radiation lengths of a lead-scintillator sandwich with

fine-granularity, two-dimensional transverse strip structure and, b) a lead glass absorber arranged in a tower structure.

The function of the inner shell in the calorimeter (the preshower sandwich) is manifold: i) the light output is sufficiently high to guarantee efficient low energy photon detection, ii) with its high granularity it provides a precise measurement of the shower center of gravity and good two shower separation, iii) it gives information on the longitudinal developement of the shower thereby substantially increasing electron/hadron discrimination, iv) it can be conveniently used in the trigger to constrain the event topology. The lead glass shell provides longitudinal shower containement and, because of its fine-grained tower structure, is essential in resolving multicluster ambiguities.

The preshower consists of a series of shells. Each scintillator shell is built with a double layer of 3 mm diameter scintillation fibers. The fibers are arranged in small grooves carved on the surface of an aluminum support structure to guarantee good uniformity. The use of scintillating fibers greatly simplifies the light collection design, an essential feature for such a compact topology. Every one of the 5 x 2 layers of parallel fibers is read by a photomultiplier; the width of the fiber bundle collected on a P.M. is determined by requiring that the bundle area should match the photocathode area. With 1.5" P.M. this width is 3.5 cm corresponding to an angular bin of 3 degrees.

The fiber characteristics [12] are summarized in Table III. With the proposed sampling structure we estimate that a minimum ionizing particle, traversing the preshower at normal incidence, should produce of the order of 75 photoelectrons in each of the two systems of fiber bundles (azimuthal and polar angle read out). About the same yield of light is expected from a 50 MeV photon converted inside the preshower.

The lead glass absorber has a pointing geometry; the choice of the element size is not critical. With a 3.5 X 3.5 cm^2 upstream face, the downstream face optimally matches a 2" P.M. photocathode area and two-shower separation is good to a few cms. We are performing a simulation of the shower developement along the calorimeter elements to compare the performance of two systems, one with 3.5 X 3.5 cm^2 (2" P.M.) and the other with 5 X 5 cm^2 (3" P.M) faces.

All calorimeter parameters are summarized in Table IV. The system, as described, is completed by a small wall of BaF_2 crystals covering the forward hemisphere from 9 degrees down to 1 degree. The choice of BaF_2 crystals is motivated by the requirement of a radiation-hard component at forward angles. Small crystals of BaF_2 will also be fit close to the interaction region, at polar angles > 70 degrees (wherever this is possible without interfering with the gas jet target structure) to detect very low energy photons from π^0 decay. Here the choice of BaF_2 is suggested by the requirement of a high light output.

7. Trigger

The pulse information from all counters is stored on fast ADCs. Whenever it will be necessary to cover a wider dynamic range, the signal will be split into two components (typically in a ratio 10 to 1) and sent to two independent ADC channels.

The detector elements entering the first level trigger are:

a) A set of 36 counters lining the outer surface of the cylindrical central detector, each 2.7 cm wide and 60 cm long, built out of 5mm thick NE110 scintillator (S_i,i=1,36). Each of the counters covers an azimuthal bin of 10 degrees.

b) The Cerenkov counters (C_i,i=1,6). The six faces of the pyramidal mirror, define the azimuthal modularity of the system ($\Delta\phi$=60 degrees).

c) The Preshower counters. The signals from the individual read out elements are ORed to define 5 degrees bins in polar angle (PT_i,i=1,12) and 10 degrees bins in azimuthal angle (PF_i,i=1,36).

d) the BaF_2 counters (BF_i) (number to be determined).

The elementary logical definitions in the fast trigger are:

a) Charged particle: $CH_i = (S_i.PF_i).OR(PT_j)$ i=1,36; j=1,12

b) Electron: $E_k = C_k.OR(CH_i)$ k=1,6; i=6k-6,6k-1

c) Photon: $G_i = PF_i.OR(PT_j).ANTI(S_i)$ i=1,36; j=1,12

d) Two body kinematics: a set of matrix conditions on the PT_i (MPT) and PF_i (MPF) designed to accept the topologies allowed by the selected final state kinematics.

e) Multiplicity $\leq$ N: on S_i (MNS)

f) Veto on BaF_2 counters : ANTI(B).

From these elements we can build, for example, a fast trigger for inclusive ψ : $E_i.E_j$.MPT.MPF or for exclusive $\gamma\gamma$ final states: $G_i.G_j$.MPT.MPF.ANTI(B).

The electronics for this level will be standard CAMAC-ECL. With the use of programmable logic units we can easily build the required logical conditions, in a time window of the order of 50 nsec, allowing for multiple simultaneous triggers.

The second level trigger (typically 1 msec), will utilize fast CAB-like processors to drastically reduce the acquisition rate by:

a) discriminating on the total energy deposited in the calorimeter to select high mass electromagnetic final states,

b) tighten the kinematical constraints on the charged final states by preprocessing the tracking information, and

c) discriminate on the topology of neutral final states with a clustering algorithm applied both to the preshower and lead glass elements.

Based again on the findings of R704, appropriately scaled to the higher luminosity, higher acceptance regime, we expect acquisition rates of the order of less then 10 events/sec.

References

1. C. Baglin et al., EP Int.Rep. 85-01, CERN

2. C. Edwards et al., Phys. Rev. Lett. 48 (1982), 70

3. M.Macri', III Lear Workshop, Tignes 1985

4. Barbieri et al., Nucl.Phys. B154 (1979),535
   M.G.Olsson,A.D.Martin,A.W.Peacock, MAD/PH/193 (Aug. 1984)
   for earlier papers see reference cited in these papers.

5. V.L.Chernyok,A.R.Zhitnitsky, Phys. Rep. Vol.112 No 34 (1984)
   E.L.Berger,P.H.Damgaard,K.Tsokos, Nordita 84/26 preprint

6. V.A. Novikov et al., Phys. Rep. Vol.41 No 1 (1978)

7. A.Billoire, Phys.Lett. 76B No 4 (1978),499

8. M.K.Gaillard,L.Maiani,R.Petronzio, TH 3235,CERN

9. W. Obert, Rarified Gas Dynamics Symposium, Cannes, France, 1978

10. C. Baglin et al., XXII Intern. Conference on High Energy Physics, Leipzig, German Democratic Republic, July 1984.

11. C. Biino et al., to be published in NIM

12. M. Bourdinaud, private comunication

TABLE I

Reaction	P_{lab} MeV/c	R704 σ^{eff} (pb)*	R704 σ^{eff}_{back} (pb)	Proposed Experiment σ^{eff} (pb)**	Proposed Experiment σ^{eff}_{back} (pb)	Acceptance Ratio
$p\bar{p}\to\eta_c\to\gamma\gamma$	3689	22-42	9-30	90-170	36-120	4
$p\bar{p}\to\chi_1\to\psi+\gamma$ $\to e^+e^-+\gamma$	5553	130	<5	650	25	5
$p\bar{p}\to{}^1P_1\to\psi+\ldots$	5600-5615	3-11	<8	15-55	40	5
$p\bar{p}\to\chi_0\to\psi+\gamma$ $\to e^+e^-+\gamma$	5727	150	<5	750	25	5
$\to\gamma\gamma$		7-17†	1-9	35-85	5-45	5
$p\bar{p}\to\psi\to e^+e^-$	4068	3000	-	6×10^4	-	5

TABLE I: Effective cross sections are defined from: Number of events/sec = $\sigma^{eff}\times L_o$, where L_o is the instantaneous luminosity. The projected values for the new experiment are scaled from the R704 ones, considering only the geometrical acceptance ratio.

* Cross sections (without background subtraction), measured at the peak of the resonance for χ_1, χ_2, ψ; average over scans for $\eta_c\to\gamma\gamma$, ${}^1P_1\to\psi+\ldots$, $\chi_2\to\gamma\gamma$. No corrections have been applied for geometrical acceptance or for detector and reconstruction efficiencies.

** An enhancement factor corresponding to the inverse ratio of the center of mass energy resolution (~4) was applied for the narrow ψ resonance. Some of this enhancement is also expected for the χ_1 resonance if the total width is 300 KeV, but has not been applied to the projected cross section.

† Compatible with the value measured by the Crystal Ball Collaboration[10].

TABLE II
Structure and size of the elements of the central detector

layer	type	# wires	Radius (mm)	Length (mm)	Remarks
A	Beam pipe	-	25	-	
B	Cathode MWPC	-	30	-	
C	Anode 1 MWPC	112	38	180	stereo -3
D	Cathode MWPC	-	46	-	
E	Anode 2 MWPC	176	54	240	
F	Cathode MWPC	-	62	-	
G	Anode 3 MWPC	224	70	315	stereo +3
H	Cathode MWPC	-	78	-	
I	Cathode DC	-	81	-	
J1	Sense DC #1	64	84.5	360	+64 field
J2	Field DC	-	88		
J2	Sense DC #2	64	91.5	360	+64 field
J4	Field DC	-	95	-	
J5	Sense DC #3	64	98.5	410	+64 field
J6	Field DC	-	102	-	
J7	Sense DC #4	64	105.5	410	+64 field
J8	Field DC	-	109	-	
J9	Sense DC #5	64	112.5	460	+64 field
J10	Field DC	-	116.5	-	
J11	Sense DC #6	96	120.5	460	+96 field
J12	Field DC	-	124	-	
J13	Sense DC #7	96	127.5	510	+96 field
J14	Field DC	-	131	-	
J15	Sense DC #8	96	134.5	510	+96 field
J16	Field DC	-	138	-	
J17	Sense DC #9	96	141.5	560	+96 field
K	Cathode DC	-	144	-	

TABLE III

FIBER CHARACTERISTICS

DIAMETER	1 - 3 mm
LIGHT OUTPUT	3 photoelectrons / mm minimum ionizing particle
ATTENUATION LENGTH	5-6 m
LIGHT TRAPPING ANGLE	25 degrees
CLADING THICKNESS	25 microns
RADIATION DAMAGE LEVEL	$> 10^5$ rad
COST	.20 $/meter

TABLE IV

PRESHOWER PARAMETERS

Number of elements	Width (cm)	Length (cm)	Angular bin (degrees)	P.M. diameter (inches)	
Azimuthal read out elements: cylindrical shell					
120	3.5	150	3	1.5	FIBERS
Azimuthal read out elements : end cap					
120	1.3-3.5	49	3.	1.5	trapezoidal scintillator (NE110)
Polar read out elements: Cylindrical shell				22 to 75 degrees	
43 X 2	3.5	188-230	.5- 3.	1.5	FIBERS
Polar read out elements: end cap				9 to 22 degrees	
14 X 2	3.5	80-230	1.	1.5	FIBERS
LEAD GLASS ABSORBER					
Cylindrical shell					
30 X 135	3.5X3.5	30		2.	SF5
OR					
15 X 70	5.X5.	30		3.	SF5
End cap					
1280	3.5X3.5	30		2.	SF5
OR					
630	5.X5.	30		3.	SF5

Figure captions

Fig.1 Mass spectrum of charmonium states

Fig.2(a) χ_1, χ_2 spectrum;
Crystal Ball data vs 3 weeks of data of R704

Fig.2(b) χ_1, χ_2 spectrum;
Crystal Ball data vs 3 weeks of data at FNAL
(proposed experiment)

Fig.3 Working principle and performance of molecular jet

Fig.4 Overall detector cross section (side view)

Fig.5 Central detector cross section: side view

Fig.6 Central detector: wire layout

Fig.7 Cerenkov counter: design.

Fig.8 Cerenkov counter: alternative design

Fig.9 Detector cross section: front view

Fig.10 End-cap pre-shower

Fig.11 Longitudinal structure of the calorimeter

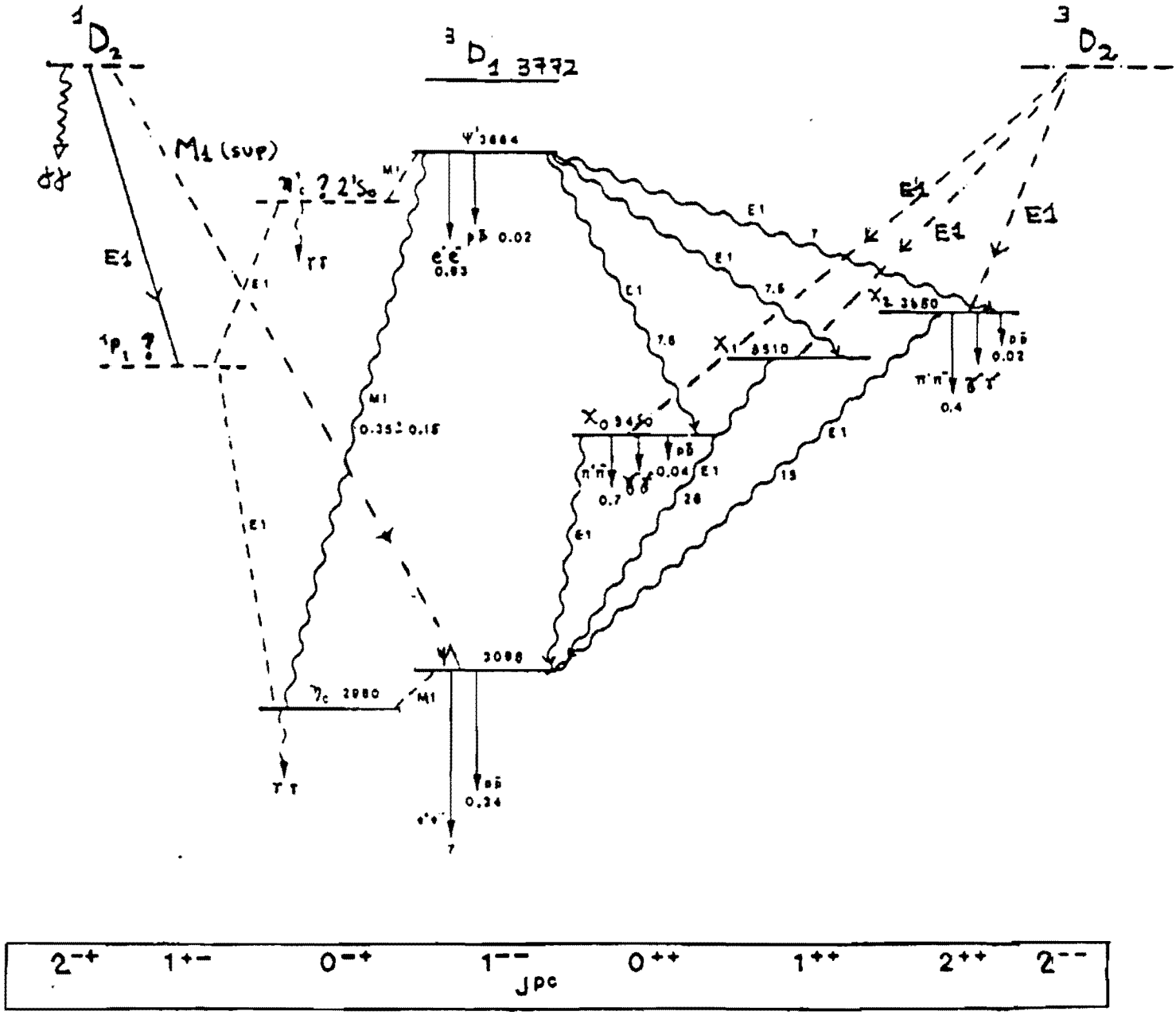

Fig.1 Mass spectrum of charmonium states

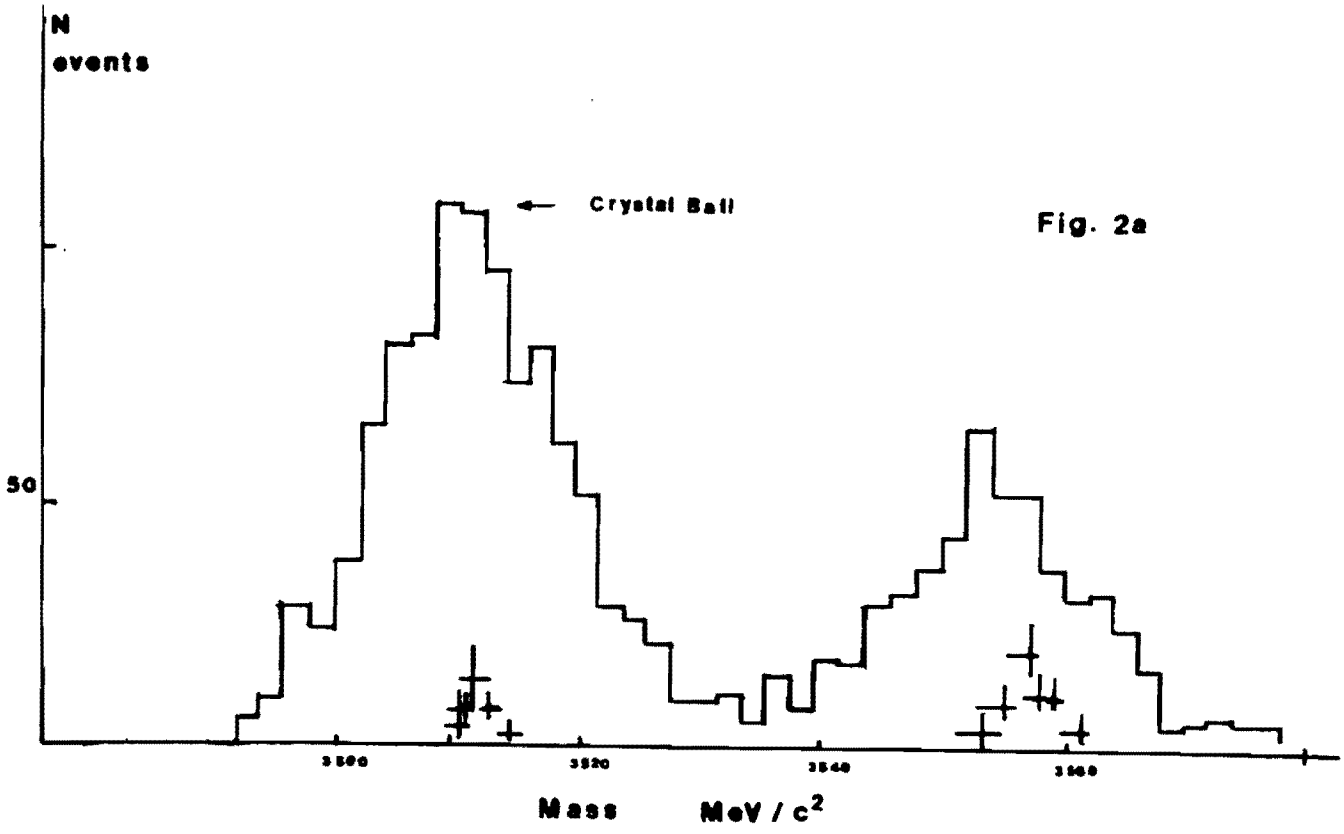

Fig.2(a) χ_1, χ_2 spectrum;
Crystal Ball data vs 3 weeks of data of R704

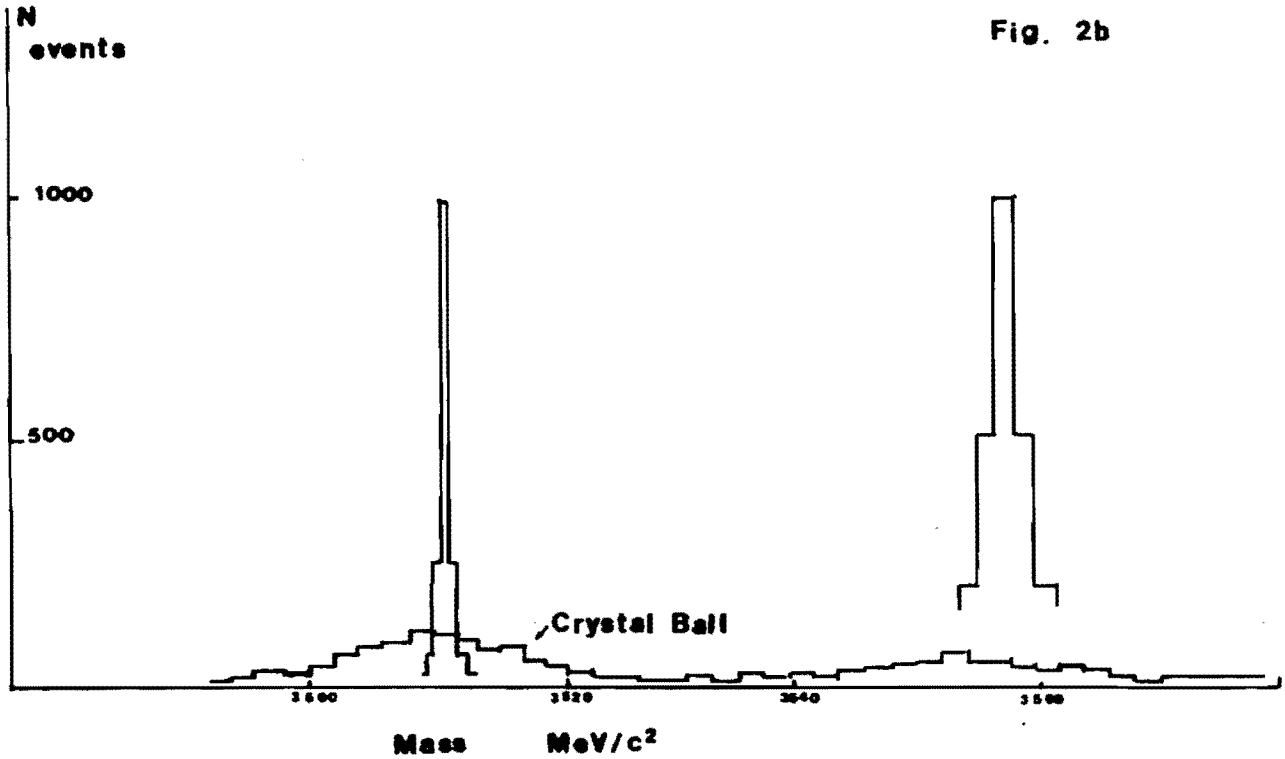

Fig.2(b) χ_1, χ_2 spectrum;
Crystal Ball data vs 3 weeks of data at FNAL
(proposed experiment)

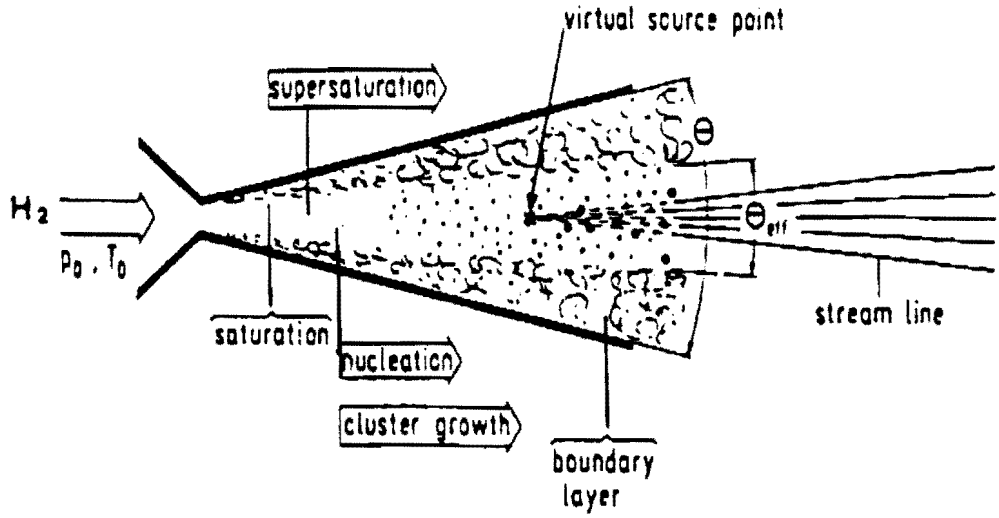

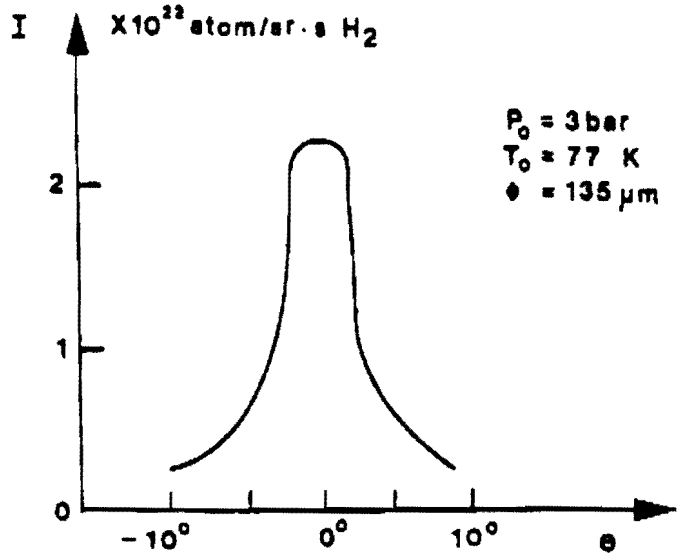

Fig.3 Working principle and performance of molecular jet

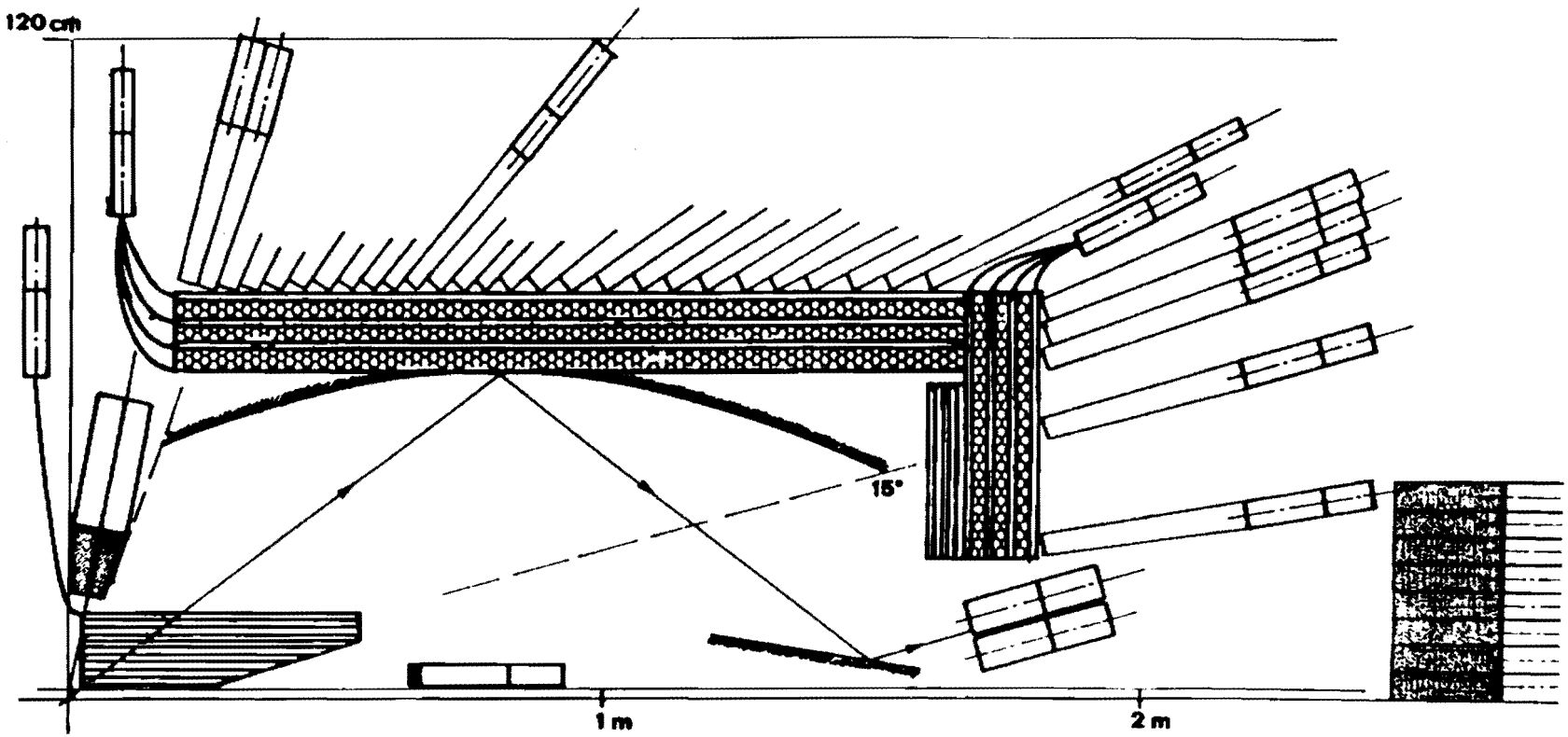

FIG. 4

Fig.4 Overall detector cross section (side view)

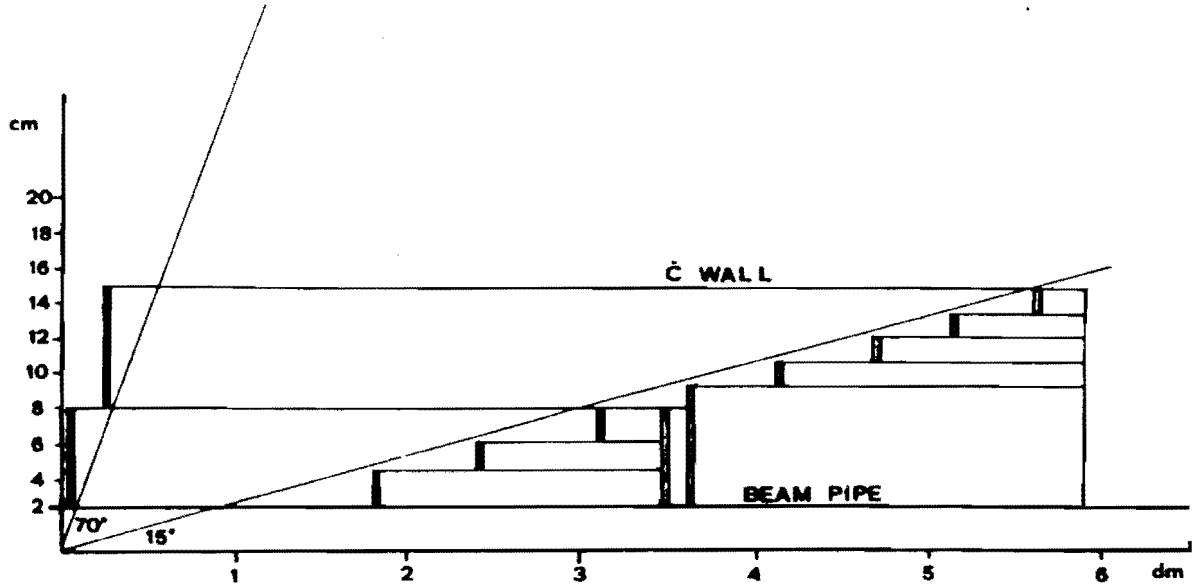

Fig.5 Central detector cross section: side view

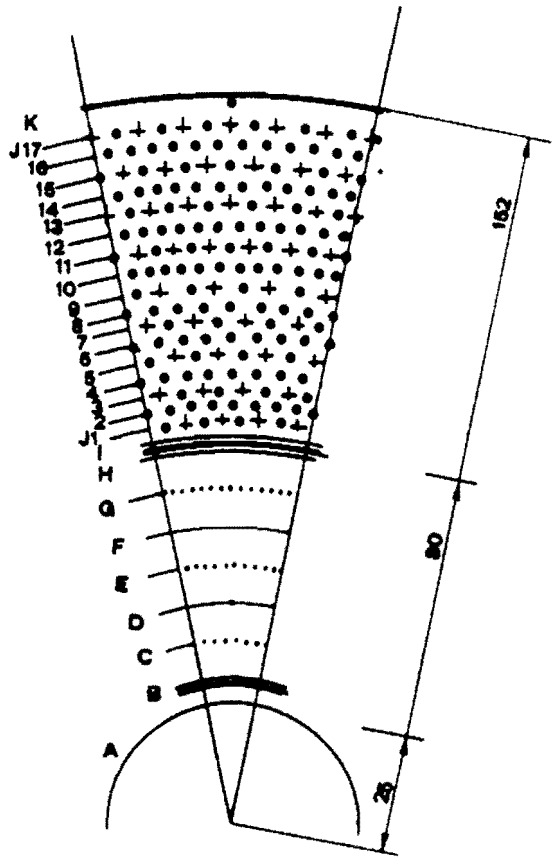

Fig.6 Central detector: wire layout

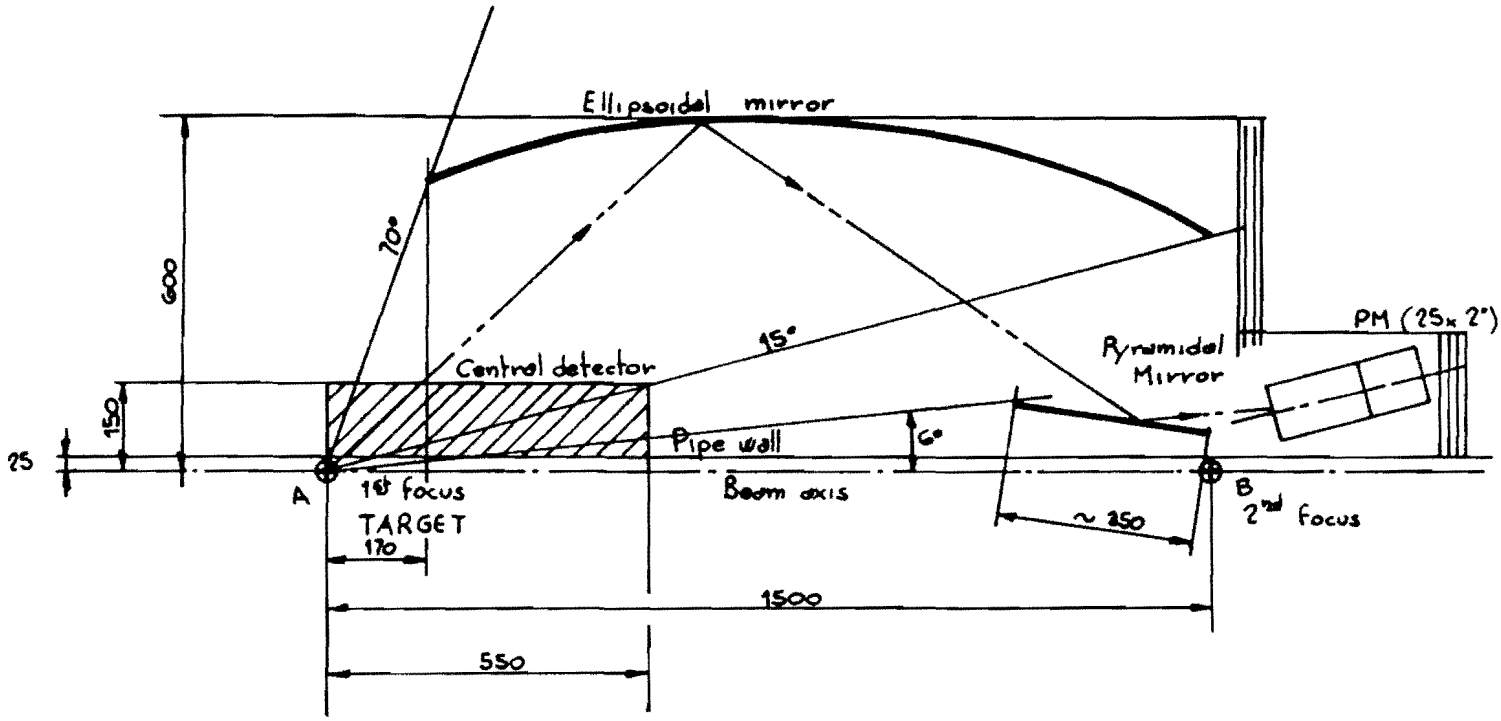

Parameters

a. 100 cm

b. 60 cm

Focus distance from center :

$$c = \sqrt{100^2 - 60^2} = 80 \text{ cm}$$

Fig.7 Cerenkov counter: design.

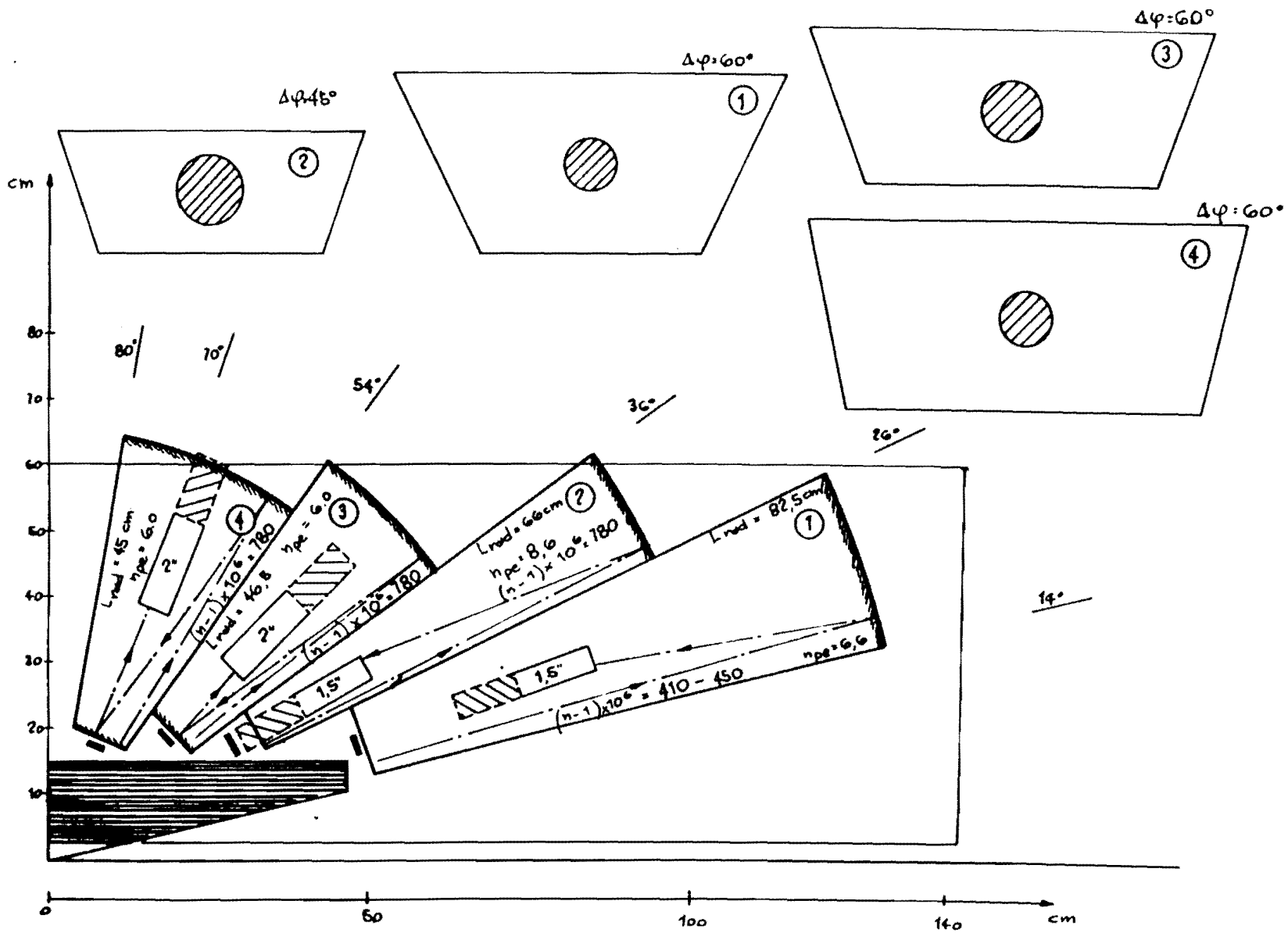

Fig.8 Cerenkov counter: alternative design

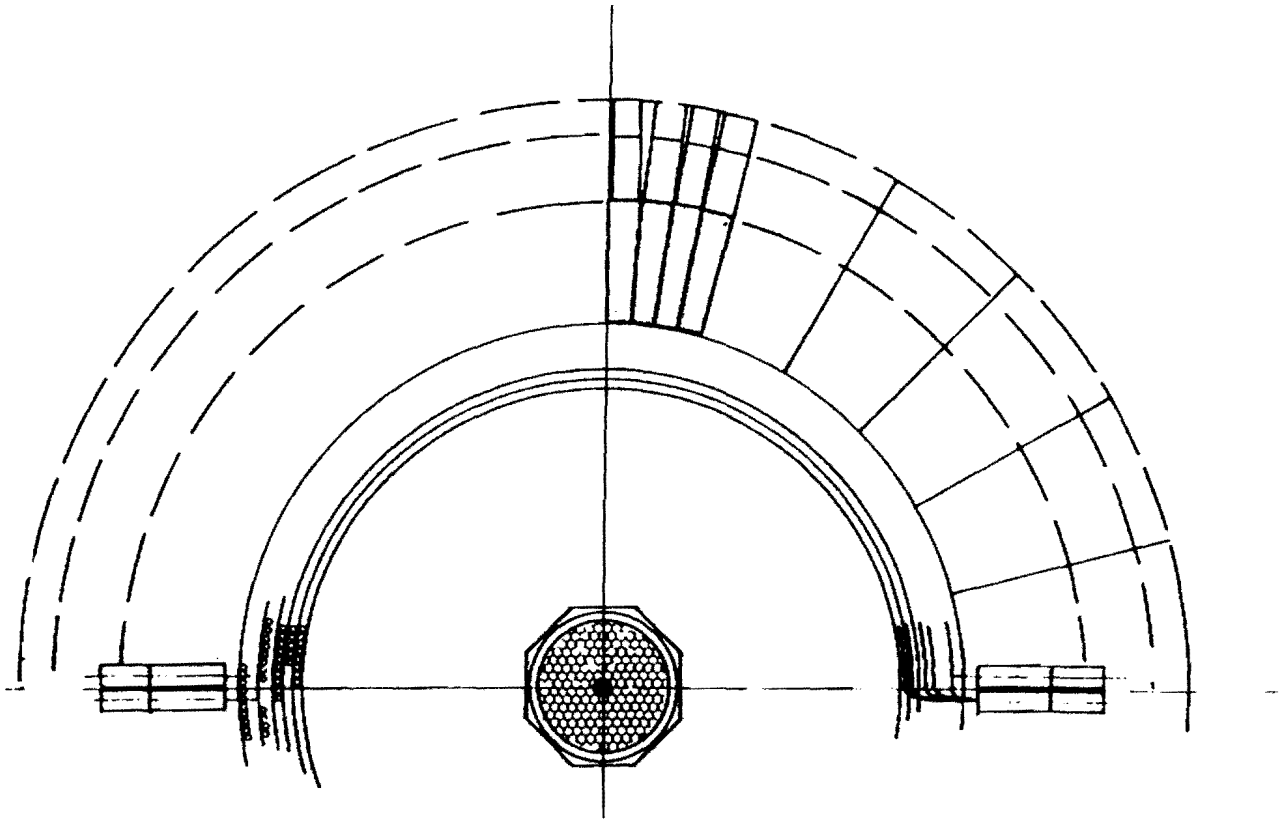

Fig.9 Detector cross section: front view

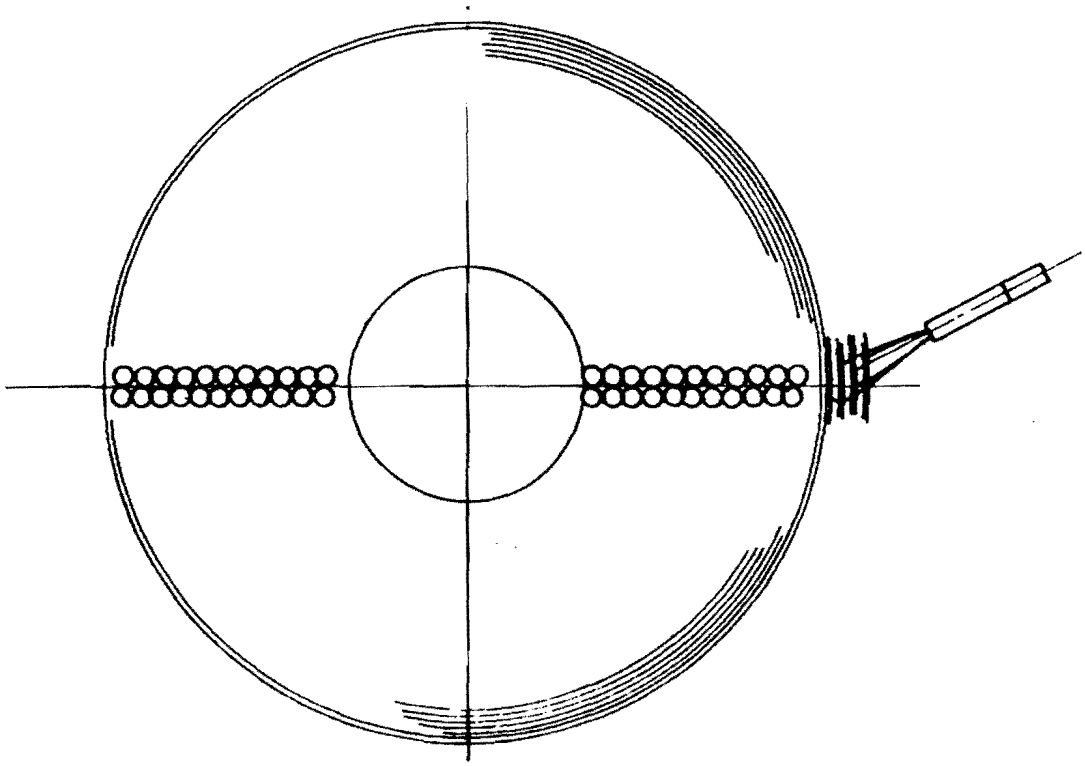

Fig.10 End-cap pre-shower

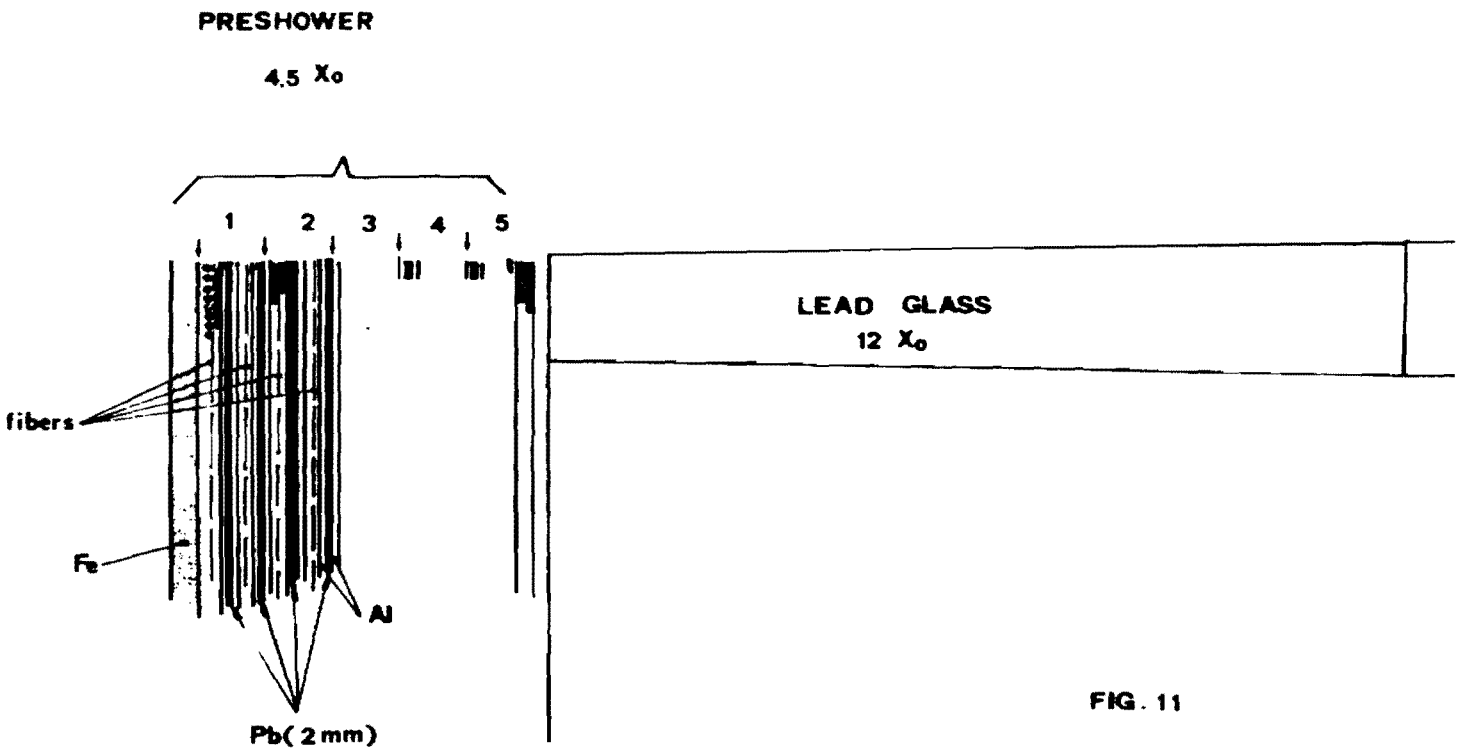

Fig.11 Longitudinal structure of the calorimeter

APPENDIX

OPERATION OF THE ACCUMULATOR

The production of final states with invariant masses in the range 2.5-3.8 GeV requires operation of the accumulator in the energy range 3.0-6.7 GeV. In order to preserve the momentum definition and the transverse emittance of the antiproton beam in the presence of the dispersive effects of the gas jet the antiprotons must be stochastically cooled. Operation of the accumulator in this mode is complicated by two effects: First, the normal transition energy of the accumulator as is 5.1 GeV. As this energy is approached the momentum compaction of the machine approaches zero and the stochastic cooling system becomes ineffective due to the lack of mixing. Second, the field quality of the accumulator magnets at the extremes of the magnet aperture deteriorates as the excitation currents are moved away from the design values for 8.89 GeV/c. As the following discussion shows neither of these effects is serious.

Transition Energy

The momentum compaction of the accumulator, η, is related to the transition gamma γ_T by, $\eta = \gamma_T^{-2} - \gamma^{-2}$. γ is the relativistic factor E/m. The transition gamma is a function of the lattice, while the momentum compaction depends both on the lattice and energy. A momentum compaction in excess of .005 is required for the stochastic cooling systems to be effective. Table A-I shows the variation of the momentum compaction, with energy for two different values of γ_T the design value of 5.46, and a value lower by one unit. As seen, our requirement on the momentum compaction would preclude operation in the center of mass energy range 3.25-3.50 GeV if γ_T could not be changed from 5.46. If one were able to lower it to 4.46 this range of center of mass energies is accessible. Thus, given the

ability to select γ_T anywhere in the range 4.46 to 5.46 makes the entire range of charmonium states accessible.

Figure A1 shows the accumulator lattice tuned to the normal parameters with γ_T=5.46 as given in the TeV I Design Report. Figure A2 shows an accumulator lattice which has been retuned to give a γ_T of 4.46 without changing either the horizontal or vertical tune of the machine. The dispersion is increased from 9.0 to 12.5 m in the high dispersion straight sections and increases from 0 to 1.6 m in the normally dispersion free straight sections. While the change in the maximum beta within the machine is minimal (from 32 to 35 m), the change in disperion in the two straight sections rules out antiproton accumulation with such a lattice. The storage and cooling of already cooled beams is feasible with this lattice. Since accumulation is done most efficiently at 8 GeV with the normal tune it is only necessary to decelerate to the operating energy and then adjust γ_T.

Magnetic Field Quality

The magnets in the accumulator and in particular the quadrupoles operate in a saturated state at the design energy of the ring (B=17KGauss in the dipoles). As a result the field shape changes significantly as the field in the magnets is lowered and the steel at the edge of the magnet aperture starts to come out of saturation. This effect precludes antiproton accumulation, which uses the full aperture of these magnets, at any other energy than the design energy of the accumulator. Beam storage at lower energies is possible as long as the beam is stored at the central momentum of the machine and has a small enough transverse emittance and momentum spread. A beam with emittance of less than 5π mm-mrad meets these requirements although this is still being investigated.

Production and Accumulation of Pbars

Antiprotons are produced, collected, accumulated and cooled at 8 GeV following the same sequence of operations as outlined in the Tevatron I Project Design Report. Antiprotons are produced by first extracting 120 to 140 GeV protons from the Main Ring at F17 and then transporting these protons to the target at AP-0 (Pbar Target Hall). The Main Ring cycle which is needed to produce pbars is expected to have a duration of 2 sec. The Main Ring cycle used to fill the Tevatron during fixed target physics can have a duration as short as 3 seconds. The principal difference lies in the fact that for a fixed target cycle (Tev II) the Main Ring is filled with 12 Booster batches whereas for a pbar production cycle the Main Ring receives only one Booster batch of $2x10^{12}$ protons.

The plan of operating the Antiproton Source during the commissioning phase takes advantage of the fact that during Tev II operation the Main Ring is dedicated to filling the Tevatron for only 3 seconds out of every 60 second Tevatron cycle. The unused 57 seconds could be used for up to 28 pbar production cycles. It is believed that the Main Ring cannot cycle during the acceleration parabola and the parabola that precedes the start of flat top. The Main Ring may have to be at 8 GeV for as much as an additional 3 seconds.

We propose to use the same operations pattern, albeit at a higher Main Ring repetition rate than is being used to commission the Antiproton Source. The sequence of operations which we propose is as follows:

1. One Booster batch of protons, consisting of 82 bunches, is accelerated in the Main Ring to 135 GeV. The bunch widths are reduced using the techniques

proposed in Tev I. The beam is then extracted at F17 and transported by the AP-1 line to the pbar target at AP-0. Up to $2x10^{12}$ protons/pulse are transported to the target.

2. A beam of negative 8.89 GeV/c particles is formed, which has a transverse emittance of 20π mm-mr in both planes and a momentum spread of 3%. When $2x10^{12}$ protons impinge on the target the resulting secondary beam is expected to contain $7X10^{7}$ pbars, $4x10^{9}$ pions, and 10^{9} electrons. The beam is transported to the Debuncher by the AP-2 line.

3. The 3% momentum spread is reduced to 0.23% by rf debunching. Since the time for the step is 10 milliseconds, the beam contains only pbars.

4. The betatron emittances are reduced from 20π mm-mr to 7π mm-mr by stochastic cooling. The initial cooling time, is .35 seconds. The cooling continues for 2.5 to 3 seconds depending on the duration of the Main Ring cycle.

5. $7x10^{7}$ pbars are transferred to the Accumulator. The beam is stochastically cooled as described in the Tev I Design Report. $7x10^{7}$ pbars are injected into the Accumulator every Main Ring cycle. The efficiency to capture pbars into the stack from the Debuncher is calculated to be >95%. The Tev I Design assumes an 85% capture efficiency, leading to an accumulation rate of $6x10^{7}$ pbars/pulse.

6. After $2.5x10^{3}$ pbar production cycles, the Accumulator will have $1.5x10^{11}$ pbars stored, corresponding to a current of 15 ma. At this point production and

accumulation stop. AP-1, AP-2, Target, and the Debuncher are turned off. The gain of the betatron core cooling systems is reduced so that the betatron emittances are no smaller than 5π mm-mr. This is a departure from pbar collection for colliding beams.

Preparation of pbars for deceleration

1. Compression of the stack tail

   Even though the accumulation stops, the Stack Tail Momentum Cooling System and the Core Cooling Systems are left on. Figure 5-16 of TeV I Design Report shows the evolution of the density, measured in particles per eV, as a function of time. It can be seen that while the bulk of the particles have been compressed into the core a few percent remain outside. In approximately 5 minutes the combined action of the stack tail system and the core cooling system pushes the pbars within 15 MeV of the center of the core. At this time the stack tail system is no longer as effective as the core cooling system in pushing the pbars deeper into the center of the core. This occurs because the noise from the stack tail cooling system tends to diffuse particles away from the center of the core. For this reason it is turned off. The gain of the betatron cooling systems are only made large enough to prevent the emittance from exceeding 5π mm-mr. Because small betatron emittances increase intrabeam scattering and thus make it difficult to compact the momentum spread, there is no gain in making the emittances smaller.

2. The core cooling system is left on until roughly 95% of the particles are

compressed to within ±1.12 MeV of the core, thereby increasing the density to 10^5 $(eV)^{-1}$. This step takes an additional 20 to 40 minutes. The pbar stack is now ready for deceleration. The peak energy density of the beam is 10^5 eV^{-1} and the betatron emittances are 2π mm-mr.

Deceleration of pbars to the collision energy

1. RF capture

A rf cavity similar to the type used for diagnostics in the Accumulator is turned on at h=10 (6 MHz) adiabatically. The core cooling system is left on until capture is complete, since the cooling system is helpful in cooling pbars into the stationary buckets. It may be useful to turn the rf on during the compression of the core step. Once rf capture is complete (>95%) the core cooling system is turned off. The rf voltage required for capture is 50 to 100 volts. Following rf capture the beam is moved on to the central orbit of the accumulator.

2. Deceleration

The rf voltage is increased to 2500 volts and the synchronous phase angle is changed to -11.5°, resulting in a decelerating voltage of 500 volts/turn. The beam energy initially decreases at a rate of 313 MeV/second. Simultaneously the dipole and quadrupole power supplies are programmed to track this change. Deceleration continues until the collision energy is reached. As η decreases the rf voltage and phase are changed in order to keep the energy decrease per turn constant. The time to reach the center of mass energy for the formation

of the 1^{++}(3510) is 11 seconds. The time to reach the 1^{--}(3069) is 15 seconds, in this case it is necessary to crcss transition.

3. Debunching

Once the collision energy is reached the beam is adiabatically debunched and the low energy Δp core cooling system is turned on. This system has it pickups centered on the central orbit in the high dispersion straight section at A-50 in order to keep the beam in the good field region of all magnets. The core betatron cooling systems are rephased for the slower revolution frequency.

Preparation for collisions

It is proposed that a 4-8 GHz system be built for this purpose of cooling the beam at low energy. Assuming that the gain is optimized the time required to cool the beam to a momentum spread of ±.5 MeV is 30 to 60 minutes when η=.006.

The gain of the horizontal and vertical betatron system is kept large enough to prevent any growth of the beam due to intrabeam scattering. There is no point allowing the beam to be any smaller than the central core of the gas jet.

Collisions

The gas jet is turned on at a density of 1.2×10^{14} atoms/cm^2. By properly selecting the gain of the betatron cooling systems throughout the accumulation and cooling sequences, the pbar beam size at the target is matched to the gas jet size. The vertical and horizontal betatron cooling system gains are increased to

compensate for the vertical growth caused by multiple scattering in the target once the gas jet is turned on. The horizontal spot size is allowed to increase somewhat since there is no advantage of keeping it small. The luminosity is 1.1×10^{31} cm^{-2} sec^{-1}. The interaction rate is 10^{6} sec^{-1}. The lifetime of the beam due to this cause is 1.5×10^{5} sec or 50 hours.

Table A-I: Momentum Compaction as a Function of Kinematic Variables for Two Values of γ_T.

Energy (GeV)	M (GeV)	(γ_T=5.46)	(γ_T=4.46)
3.00	2.30	-.064	-.048
3.50	2.89	-.038	-.022
3.75	2.97	-.029	-.012
4.00	3.04	-.021	-.005
4.25	3.12	-.015	.002
4.50	3.19	-.010	.007
4.75	3.27	-.005	.011
5.00	3.34	-.002	.015
5.25	3.41	.002	.018
5.50	3.48	.004	.020
5.75	3.54	.007	.023
6.00	3.61	.009	.025
6.25	3.67	.011	.027
6.50	3.74	.013	.029

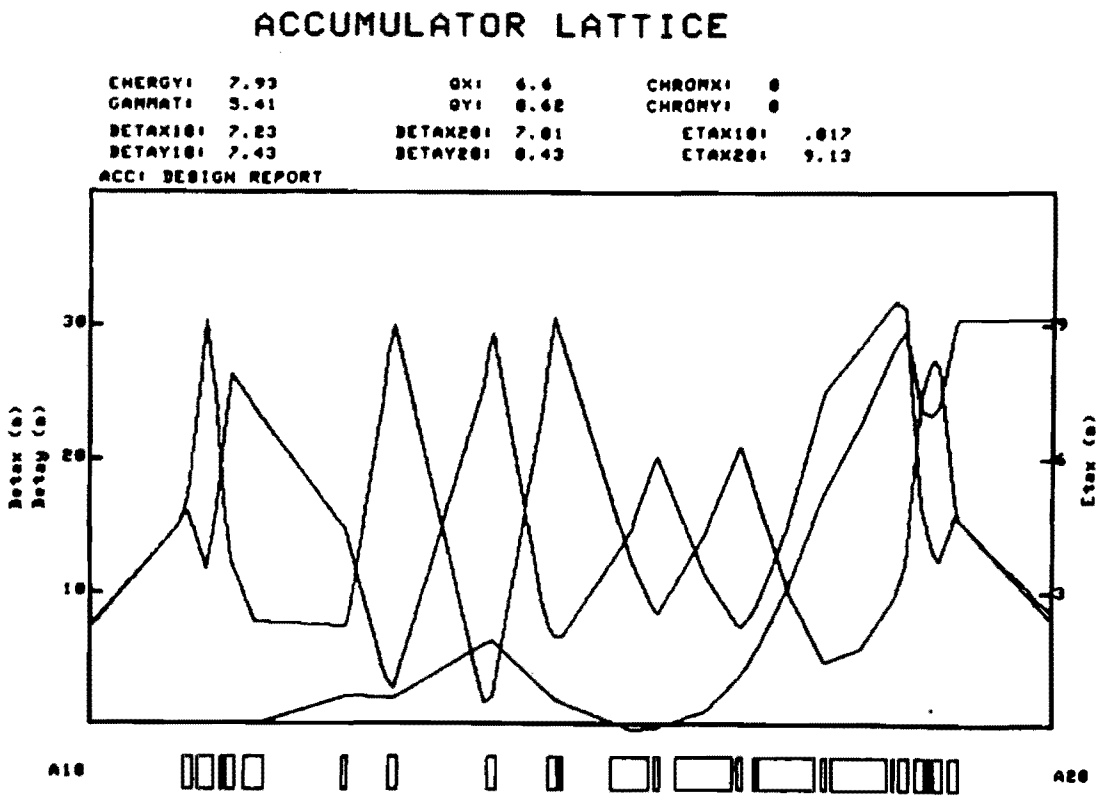
ACCUMULATOR LATTICE
ENERGY: 7.93
GAMMAT: 5.41
QX: 6.6
QY: 8.62
CHROMX: 0
CHROMY: 0
BETAX10: 7.23
BETAY10: 7.43
BETAX20: 7.01
BETAY20: 8.43
ETAX10: .017
ETAX20: 9.13
ACC: DESIGN REPORT
Betax (m)
Betay (m)
Etax (m)
30
20
10
A10
A20

Fig. A1

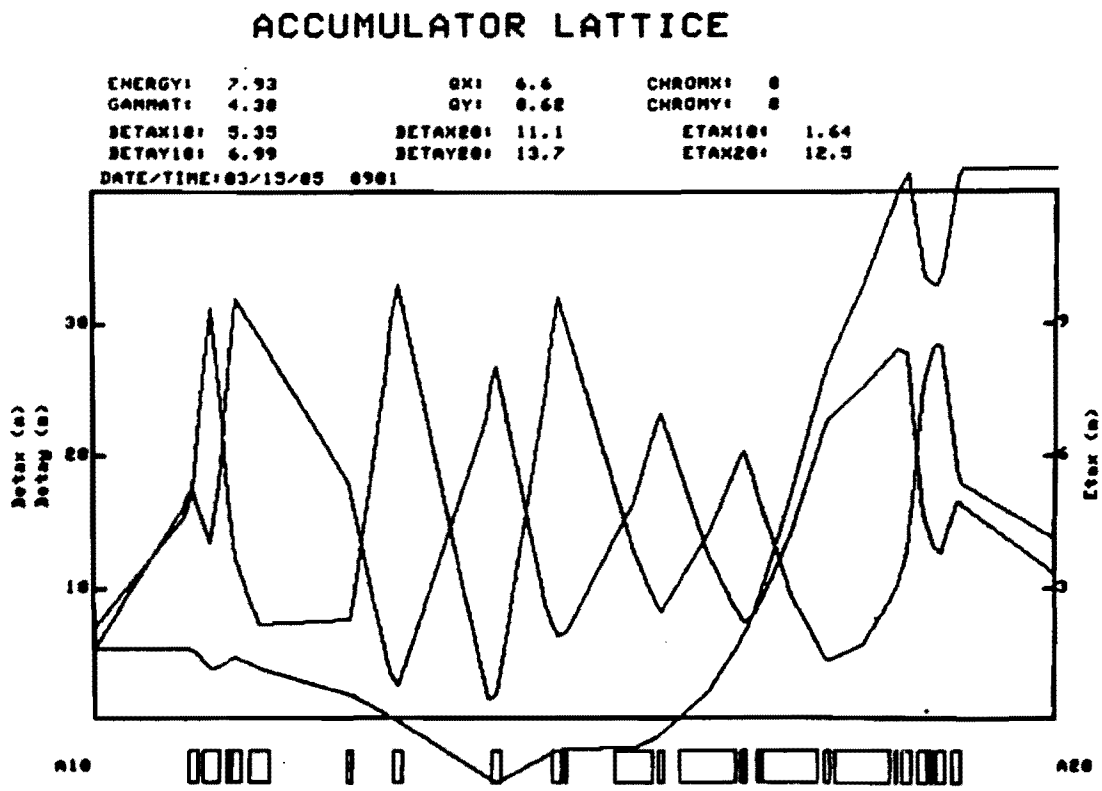
ACCUMULATOR LATTICE
ENERGY: 7.93
GAMMAT: 4.38
QX: 6.6
QY: 8.62
CHROMX: 0
CHROMY: 0
BETAX10: 5.35
BETAY10: 6.99
BETAX20: 11.1
BETAY20: 13.7
ETAX10: 1.64
ETAX20: 12.5
DATE/TIME:03/15/85 0901
Betax (m)
Betay (m)
Etax (m)
30
20
10
A10
A20

Fig. A2

ADDENDUM TO P760

As requested by the PAC we give a more detailed description of the detector, and a cost estimate. We do not claim to present here the final version, however the design should be close enough to the one that will be adopted for the cost estimate to be realistic.

A major constraint in the detector design comes from the space limitations in the Antiproton Source Enclosure. We have designed a detector which fits in a cylinder of a radius 120 cm, coaxial with the beam line. This will require the excavation of a pit in the floor of the tunnel as described in the proposal, but will not otherwise disturb normal maintenance activities (such as magnet replacement etc.).

For the central detector and the Cerenkov counter we base the cost estimates on the design sketched in the proposal (solution A for the Cerenkov).

For the gas jet target we have made a preliminary study which is based on the experience acquired in the construction and operation of the jet for R704. The choice of the pumping elements and their arrangement takes into account the space constraints at the Antiproton Source Enclosure. It appears that the clearance requirements can be met with ease.

The calorimeter

To clarify the guidelines for the design of the calorimeter we review briefly the crucial tasks that are to be performed by this part of the detector.

Reactions:

$$p + \bar{p} \rightarrow \eta_c \rightarrow \gamma + \gamma \qquad (1)$$
$$\eta_c' \rightarrow \gamma + \gamma$$

The identification of this process and the ability to separate it out from the main background reaction:

$$p + \bar{p} \rightarrow \pi^0 + \pi^0 \quad , \quad \pi^0 \rightarrow \gamma + \gamma \qquad (2)$$

rests completely on the calorimeter performance.

Two topologies of π^0 decay are particularly troublesome:

-- symmetric decays: the opening angle of the two photons is minimal. The detector must be designed to separate out the two photon clusters.

The profile of the calorimeter has been chosen so that the distance (d) between the impact points of the two γ's arising from the π^0's of reaction (2) is always $\geq$ 8 cm. In order to resolve with good efficiency the two photon clusters, we require a transverse segmentation with a typical dimension $a \leq d/2$, optimally achieved with a pointing geometry.

-- asymmetric decays: the forward photon, emitted close to the π^0 direction, carries most of the π^0 energy while the backward going photon is emitted at large angles to the π^0 direction with very low energy. A good rejection of this kind of background relies on the capability to detect low energy photons over the full solid angle and/or to measure precisely the direction of the high energy photon.

The additional requirements are then: high light output, and low energy threshold over the full solid angle.

Reactions:

$$
\begin{aligned}
p + \bar{p} &\to \chi \to \psi + \gamma \quad , \quad \psi \to e^+ + e^- \\
p + \bar{p} &\to {}^1P_1 \to \psi + \pi^0 + \pi^0 \quad , \quad \psi \to e^+ + e^- \\
&\to \psi + \pi^0 \quad , \quad \psi \to e^+ + e^- \qquad (3) \\
&\to \psi + \pi^+ + \pi^- \quad , \quad \psi \to e^+ + e^-
\end{aligned}
$$

The calorimeter should contribute to the h/e discrimination power and allow the measurement of the energy and the direction of photons produced in association with the ψ.

A rough longitudinal segmentation and/or good energy resolution helps in separating hadrons from electrons. Since a very high rejection factor is achieved with the threshold Cerenkov, we rely on energy measurements to improve on this rejection factor.

Based on these considerations we have designed a calorimeter incorporating three separate structures:

(a) A tower structure with pointing geometry (central calorimeter) with complete azimuthal coverage and extending in polar angle from θ=12° up to θ=70°. This corresponds typically to an acceptance of about 60% for the reaction:

$$p + \bar{p} \to \eta_c \to \gamma + \gamma$$

(b) A forward end plug extending in polar angle down to ~1°. This structure has a planar geometry and is built from assemblies of 3 X_0 scintillator/lead sandwiches with x,y strip segmentation, interleaved with planes of limited streamer tubes with cathode strip read-out.

(c) A system of short (6-7 X_0), high light output towers, closely surrounding the target region, to signal energy deposition at large angles. The detailed design of this structure will not be given here since it depends strongly on the exact details of the target design.

(a) The central calorimeter

We discuss the following aspects of the central calorimeter:

1. The choice of suitable components to manufacture the towers
2. The geometrical layout of the system
3. The mechanical support (Fig. 2)
4. The read-out scheme

1. In summary the requirements are: high light output, short radiation length, small time constant, and reasonable cost.

We propose the two following solutions:

-- Scintillating glasses. At present the difficulty with this choice (SCG1-C of Ohara) lies in the rather large radiation length (4.3 cm) for this material which limits the angular region where it can be used and still lie within the 120 cm radius cylindrical boundary of the detector ($\leq 38°$). Ohara and other manufacturers are however now trying to develope shorter radiation length glasses (2.5-3 cm).

The scintillation time constant (about 70 nsec) is sufficiently small. With an expected rate of 1 MHz spread over a highly segmented system we do not anticipate significant pile up-problems.

-- Lead glass/scintillator sandwich. Since this technique is fairly new and has not yet been used in any experiment we can only refer to the relevant literature [1], and summarize the results obtained with a 12 X_0 prototype (1 X_0=3.2 cm):

light output relative to SF5 : x9.5
energy resolution : $\sigma(E)/E=9.1\%/\sqrt{E(GeV)}$
time constant : 2.4 nsec (NE102)

We are planning a test to study the detection efficiency for low energy (60 MEV) photons using the same prototype. Clearly a technique must be developed to mass produce these counters.

The cost of one tower, as estimated from its components, is about 100 $ (55 $ of lead glass, assuming conservatively [1] the price to be 75 % of that of a polished block of the same volume; NE102 scintillator, 44 $). We allow a 50 % increase in their cost to account for manufacturing costs.

In summary we have 3 options:

i) use lead glass/scintillator sandwich towers over all the angular aperture

ii) use the sandwiches for $\theta > 38°$ and scintillating glass at smaller angles

iii) if a low X_0 (3 cm) scintillating glass is succesfully developed, use this over the full angular aperture.

The detailed design of geometry and mechanics and the costs estimate are based on solution (i).

2. The geometry of the system is shown in Fig. 1 and the segmentation characteristics are given in Table I. The basic criteria wich lead to this design are:

-- a compromise solution between the choice of a small number of different block shapes (5 in our design) on one side and the requirement of small deviation from pointing geometry and of good coverage of azimuthal angle ($\leq$ 5% lost in cracks) on the other side

-- the blocks have the shape of a truncated pyramid with trapezoidal bases. The downstream face of the blocks matches well with a 2 inch PM. This results in a transverse segmentation adequate to resolve two photon clusters from symmetric π^0 decays and to determine with the required accuracy (Δx(c. of g.) similar to Δx(target)) the centre of gravity of showers. The length of the blocks given in

Table I is only illustative; the final values will be determined after extensive tests of the trasmission characteristics and energy resolution vs. length, on prototypes with the correct transverse geometry. The calorimeter is segmented in 5 polar angle (θ) regions (corresponding to the 5 different block shapes); each θ region is segmented in 8 boxes with 45° acceptance in azimuth. These boxes are the structural elements of the calorimeter to which we will refer in the description of the mechanical structure.

3. A total of 40 boxes, with open entrance windows, will contain the counters, each box being longitudinally supported by steel T-beams connecting together all the boxes at a given azimuth. A large aluminum tube (diameter = 120 cm, thickness = 0.5 cm) will be used both as a radial support and reference surface for 32 of the 40 boxes; the tube will be attached at both ends to flanges, each flange being connected by steel spokes to a large wheel, rolling on a number of bearings fixed to the floor, and connected to the longitudinal T-beams holding together the boxes. In this way, it will be possible to rotate the whole structure around the vertical direction, as needed for installation and cabling of the 'down' boxes (whose final position will be inside the pit, below the floor level). The last 8 boxes, corresponding to the forward acceptance down to 12°, will be sitting on a special support, shaped as a truncated cone connecting on one side to the second large wheel, and on the other side to a third, smaller wheel at the end of the calorimeter volume. A conventional motorized gear coupling system will provide power to rotate the calorimeter at installation time. Based on this mechanical scheme, the total time needed to assemble the support and install the calorimeter is estimated to be about 20 days; the cost of the support is estimated as about 100 K$.

4. The particle energy that we should detect ranges from less than 50 MeV to

about 5 GeV. With 10^4 photoelectrons/GeV we expect that a minimum ionizing particle and a 50 MeV photon will give respectively 1500 and 500 photoelectrons (pe).

Requiring a lower detection threshold of 100 pe sets the PM gain to $2\text{-}3\times10^5$. Phototubes which can be operated at this gain level, with a linearity regime extending up to 5 GeV particle equivalent current, are not hard to find (see for example XP3202B or XP2202B). Based on preliminary discussions with Phillips rapresentatives we estimate that a PM/base assembly can be obtained at a cost of 100 $ per unit.

By using twisted-pairs flat cables for individual PM signals, we should be able to reduce the number of cables (with some redundancy) to about 5/box + one from the HV supply, with a possibility of using the same voltage for all the tubes in a box, just by selecting tubes with similar gain.

These cables will be terminated in nearby racks, where splitters and adders will be located (see trigger section). Twisted pairs signal lines will also carry the PM signals as well as the sum signals to the counting room (about 2500 PMs, 400 first level sums, 50 second level sums).

The signals will be digitized using 12 bits ADCs to match the expected dynamic range. The price estimate given is based on the choice of high density Fastbus modules from LeCroy.

(b) The forward calorimeter

It should be understood that this part of the calorimeter is outside the polar angle range (15-70°), which defines the geometrical acceptance for ($c\text{-}\bar{c}$) two body final states.

It has however two important functions:

-- for two body exclusive final states ($\psi \to e^+e^-$, $\eta_c \to \gamma+\gamma$) it will veto events with extra energy deposition at a polar angle $\leq 12°$

-- for multibody final states of the type $\psi+X$ it will provide energy and direction information on the extra particles produced in association with the ψ in the forward direction.

We have therefore designed a detector with a reasonable low threshold for γ detection (about 80 MeV [2]), and acceptable precision in position and energy measurement. Because of the long lever arm it will allow for an excellent angular measurement for both charged and neutral particles coming from the interaction region (about 1-3 mrad).

Other characteristics are: low cost, a straightforward support mechanism, and sufficiently small size to fit above the enclosure floor level.

Its overall characteristics are:

-- Geometry: planar, normal to the beam

-- Material: lead/scintillator sandwich:

-- Sampling: 5 mm NE102, 2 mm lead

-- Longitudinal segmentation: 5 times 3 X_0 modules for a total of 15 radiation lenghts

-- Transverse segmentation: 6 cm wide strips with x (horizontal) and y (vertical) orientation. x and y strips alternate along the z (beam) direction

-- Read-out: all strips of a set (6 cm wide, x or y) from a 3 X_0 module are coupled with lucite lightguides to a single 2" PM. To increase the precision on position measurement, strips from adjacent modules are offset by half a strip. The y strips are read from above.

The calorimeter is segmented in two parts at the x=0 plane. The x strips from

the two parts are read respectively on the left and right end of the calorimeter.

Four planes of limited streamer tubes with u (+45°) and v (-45°) strip read-out interleaved with the lead/scintillator module, are placed respectively after 0,3,6, and 9 radiation lenghts. Their principal function is to resolve ambiguities in multiple hit topologies and track charged particles. We have in mind the use of plastic streamer tubes "a la Mont Blanc" [3] with tube cross section of the order of 1 cm^2 and digital strip read out (strip width and pitch tipically 8 and 1 cm). The rate on these chambers is not expected to exceed the maximum sustainable, with negligible efficiency loss, of about 10^6 / (s m^2).

Trigger

(a) Charged trigger

As the first trigger element we plan to have a cylindrical scintillator hodoscope surrounding the central detector providing azimuthal information for charged tracks with 8° segmentation. Small 1/2" PMs (like Phillips PM1911) will be used to read out these counters.

The fast signal from the Cerenkov will be used to select electrons at the trigger level.

To improve the trigger selectivity, we would like to make use of the calorimeter information, which is fast, by summing up counter signals in each box, to obtain a 'strip-like' geometry both in θ and ϕ. This will require a splitting of the PM current (ratio 9:1 seems apropriate) between the ADC's and the trigger logic.

We propose the following scheme for the calorimeter trigger:

-- sum up signals from 6 counters in a box at a given polar angle (θ); this is the basic cell for further regrouping (first level sum)

-- add together 16 sums at fixed θ, obtaining 27 'θ-strips'

-- in parallel, add together 27 sums at fixed ϕ, forming 16 'ϕ-strips'

Standard ECL fast logic will be used to form the final trigger signal.

(b) Neutral trigger

We propose to split the neutral trigger in two levels. For the first level the same logic will be used as for charged trigger, with one important modification: the scintillator hodoscope will be set as a veto, to reject charged tracks. Elements of the forward and backward calorimeters will also act as a veto.

The 27 second level sums corresponding to "θ strips" will be digitized by 8 bit flash ADCs to obtain a fast (about 100 nsec) energy measurement. Utilizing this information, a dedicated microprocessor will provide a second level energy filter (1 msec).

Based on the R704 experience, we consider this second level trigger of crucial importance for background rejection in neutral final states.

References

[1] Cozza et al.,N.I.M. 215 (1983), 89-92

[2] As measured with a similar detector in R704

[3] E. Iarocci,N.I.M. 217(1983),30-42

Cost estimate

-- Target --

Production stage: support for H_2 injector	7500 $
evacuation chambers (with flanges)	15000 $
4 turbomolecular pumps 3500 l/s	60000 $
'root' pumps 3000,1000,250 m^3/h	35000 $
rotary pump	3500 $
VAT valves for production and recovery systems	25000 $
vacuum and ultra high vacuum measurement device	7500 $
H_2 injection circuit	15000 $
N.E.G. getter pumps	6000 $
Recovery stage: evacuation chambers	12500 $
N.E.G. getter pumps (1200 l/s)	100000 $
high vacuum measurement devices	5000 $
power supply for N.E.G. getters	7500 $
control electronics	12500 $
total	312000 $

-- Central Detector --

mechanics	35000 $
read-out	40000 $
total	75000 $

-- Cerenkov --

elliptical mirror mould	30000 $
6 elliptical mirrors	6000 $
mechanical support and alignemet controls	10000 $
12 PM (Hamamatsu R1332)	10632 $
total	56632 $

-- Calorimeter --

Central:	
lead glass/scintillator modules (150 $ each)	367200 $
2" PM + base (e.g. XP3202B; 100 $ each)	244800 $
mechanics	100000 $
cables	60000 $
power supplies (40)	80000 $
ADC system and Fastbus crates	150000 $
total	1002000 $
Front :	
scintillator (360 Kg)	72000 $
2" PMs + base	20000 $
tubes	2000 $
tubes read-out	10000 $
total	104000 $

-- Trigger --

scintillators + light guides + PMs	5000 $
electronics :	
adders (about 500)	10000 $
logic (20 ECL modules)	60000 $
total	75000 $

-- Total --

target	312000 $
central detector	75000 $
Cerenkov	57000 $
central calorimeter	1002000 $
front calorimeter	104000 $
trigger	75000 $

	1625000 $

-- Data acquisition --

VAX-750	120000 $
1 extra tape device	9000 $
2 printers	10000 $
4 terminals	10000 $
1 disk unit	12000 $

	161000 $

A tentative division of responsibilities and sharing of expences

U.S.A. groups		
Mechanics of central calorimeter	100000 $	-*-
ADC system	150000 $	
Trigger electronics	70000 $	
50 % of lead glass/scint. modules	306000 $	-*-
Data acquisition	161000 $	
Total	787000 $	
Italian groups		
Target	300000 $	-*-
Central detector	75000 $	
Cerenkov	56000 $	-*-
Forward calorimeter	104000 $	
50 % of lead glass/scint. modules	306000 $	
Total	841000 $	

-*- Responsibility for construction

Time schedule

July-October 1985	(1) Feasibility study of pit excavation in the Antiproton Source Enclosure (2) Prototype studies (Cerenkov, lead glass/scintillator modules) (3) Finalized detector and target design
November 1985	P.A.C. final decision (?)
if OK	Start target construction
Spring 1986	Pit excavation
1986	Detector construction
1987	Detector Instalation, Running (?)

TABLE I

Box type	θ min	θ max	Length [cm;X_0]	a Back face [cm]	a Front face [cm]	b Back face [cm]	b Front face [cm]	θ span	#Blocks	Weight [Kg]
1	54.5	70.0	40.;12.5	5.8	3.6	5.8	3.6	3.1	65	195
2	41.0	54.5	45.;14.	5.8	3.7	5.7	3.8	2.7	65	221
3	30.0	41.0	47.;15.	5.8	4.0	5.8	4.1	2.2	60	228
4	21.5	30.0	50.;16.	5.6	4.1	6.0	4.3	1.7	55	237
5	12.0	21.5	50.;16.	5.6	4.1	5.6	4.3	1.35	61	246

General information:
- 2448 counters
- Radiation length : 3.15 cm
- Density : 3.4 g/cm³
- 5 different counter sizes, all counters shaped as truncated pyramids with trapezoidal bases

```
...
!  !..
!     !..
!     !  !...
!     !     !
!     !<- b !
!     !   ..!
!     !..!
!   ..!
!..!     ↑
         !
         a
```

FIG. 1

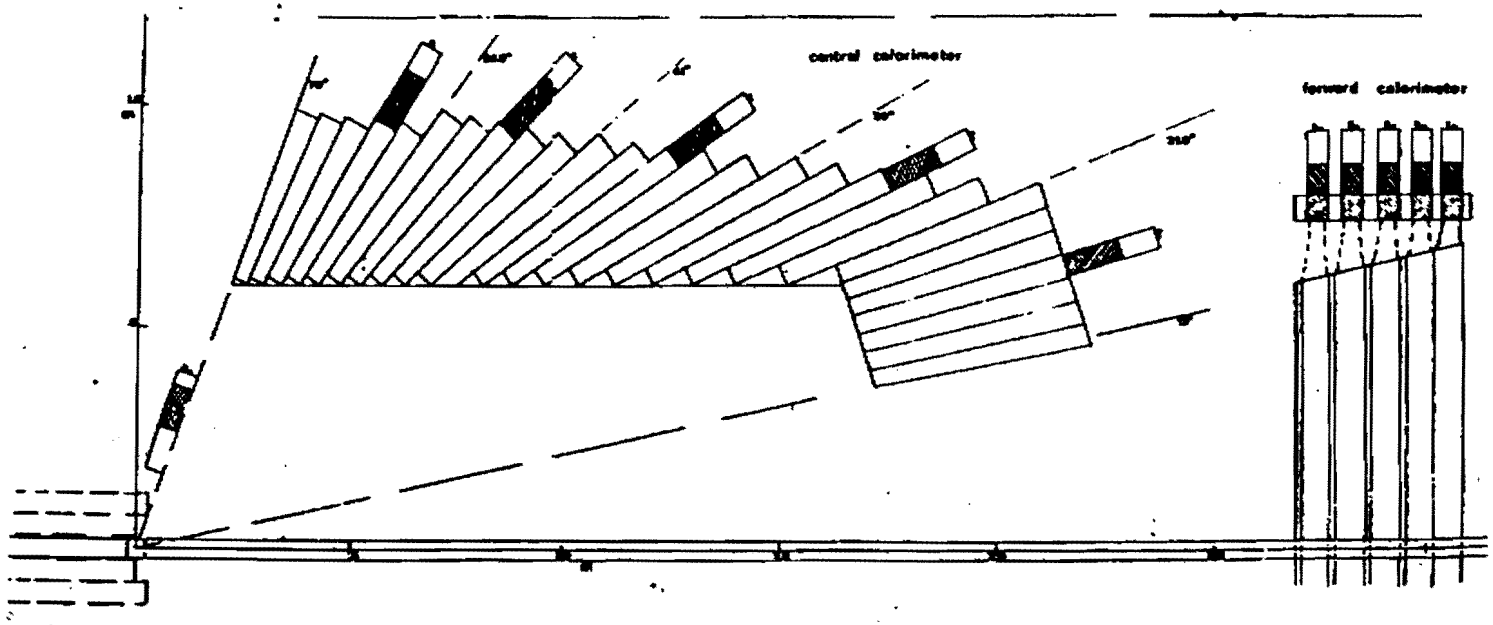

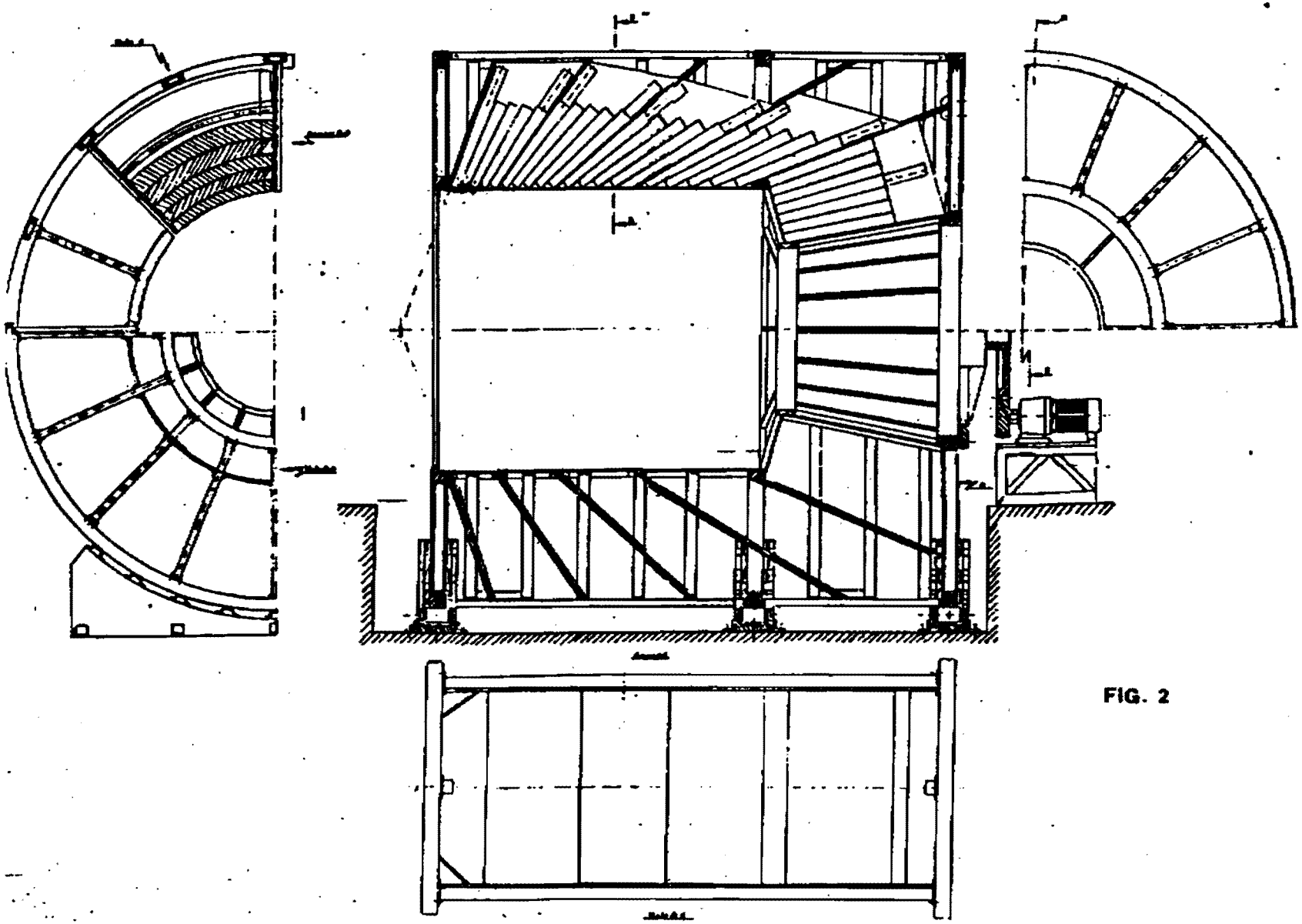

FIG. 2

Fermilab

June 2, 1985

Dr. Leon M. Lederman
Director's Office

Dear Leon,

I am enclosing an addendum to Proposal 760 ('A Proposal to Investigate the Formation of Charmonium States using the Pbar Accumulator Ring'). In this addendum we attempt to answer some of the questions that were raised in the last PAC meeting.

I wish to bring to your and the committee's attention the cost estimate included in this addendum. The detector design has not completely crystalized in our minds and thus the presented estimates should be evaluated with this in mind. It is my belief that the estimate presented sets the overall scale of the proposed experiment. In addition I wish to point out that the estimate is also somewhat incomplete, e.g. the backwards calorimeter has not been included.

Another point that I wish to stress is that a clear indication from the PAC as to the fate of this proposal at the June meeting would be a great help for the Italian members of our collaboration. Such an early reply from the PAC will allow them to submit their request to the appropriate financing authorities of their country by July and to receive a decision by September.

The addendum is the work of our Italian collaborators, our part of the collaboration has not had the opportunity to completely scrutinize it; after all the antiproton source is absorbing all our efforts.

Sincerely,

Petros Rapidis

P.A. Rapidis
Tevatron I Section

PAR:mjb

Enclosure

cc: J. Peoples
R. Cester, Torino
P760 Collaborators

ADDENDUM 2 TO PROPOSAL P760

A PROPOSAL TO INVESTIGATE THE FORMATION OF CHARMONIUM STATES USING THE PBAR ACCUMULATOR RING

V. Bharadwaj, J. Griffin, J. Hangst, W. Kells, J. McCarthy

J. MacLachlan, J. Marriner, W. Marsh, J. Peoples

P. Rapidis, D. Young

Fermi National Accelerator Laboratory

R. Calabrese, P. Dalpiaz, P. Ferretti-Dalpiaz, E. Lupi,

F. Petrucci, M. Savrie

Universita' di Ferrara

M. Mainelli, M. Mattera, F. Tommassini, V. Valbusa

Universita' Di Genova

C. Biino, G. Borreani, R. Cester, E. Menichetti, S. Palestini,

N. Pastrone, G. Rinaudo, L. Tecchio

Universita' di Torino

Spokesperson : R. Cester

Local contact: P. Rapidis

December 12, 1985

December 10, 1985

The PAC has asked us to discuss in some detail the two channels

(1) $\bar{p}+p\rightarrow\eta_c\rightarrow\gamma+\gamma$

and

(2) $\bar{p}+p\rightarrow{}^1P_1\rightarrow J/\psi+\pi^o+\pi^o$

as examples of the adequate performance of the proposed detector. We have organized this discussion in four steps: a) the evaluation of the cross section and/or cross section limits, b) the identification of the main background components, c) an estimate of the signal to background ratio to be obtained with the proposed detector and d) the integrated luminosity requirements. These four steps will be discussed separately for the η_c and the ${}^1P_1$. Whenever possible the cross section limits and background estimates are based on the findings of experiment R-704 at the ISR[1]. Monte Carlo techniques have been used, when needed, to extrapolate to the proposed experimental set up and to integrate missing information.

1. η_c production

a) Cross-section Estimate:

By writing the cross section for reaction (1) in the form shown in (3) its dependence on experimentally measured quantities can be shown explicitly.

(3) $\sigma(m_{\eta_c})=\pi(\hbar c/p)2(\Gamma(\eta_c\to\gamma\gamma)/\Gamma tot)(BR(\eta_c\to\bar{p}p))$

The relevant experimentally measured quantities are:

$BR\ (\eta_c\to pp) = 1.1\pm.04\pm.05\ 10^{-3}$ 2)

$m\ (\eta_c) = (2984\pm4)\ MeV/c^2$ 3)

$\Gamma_{tot}\ (\eta_c) = 11.5\pm4.5\ MeV$ 3)

The only unknown piece of data needed to evaluate (3) is $\Gamma(\eta_c\to\gamma\gamma)$, which can be estimated from the partial width of the ψ decaying to e^+e^-, $\Gamma(\psi\to e^+e^-)$.

(4) $\Gamma(\eta_c\to\gamma\gamma)\Gamma(\psi\to e^+e^-) = 4/3$

According to (4) using 4.7 keV for $\Gamma(\psi\to e^+e^-)$ we estimate $\Gamma(\eta_c\to\gamma\gamma)$ to be 6 kev and note that it is consistent with the experimental limit of 7 kev (95% confidence). Using these numbers we obtain a value of .54 nb for the cross section at the resonance peak.

Since the central calorimeter is designed to detect γ rays emitted at laboratory polar angles between 12° and 71°, the geometric acceptance for detecting both γ rays simultaneously is 62%. On the basis of experience with the $\pi^o\pi^o$ data from R-704 only those events for which $|\cos\theta|<.55$ will be used in the η_c sample, thereby reducing the acceptance to 55%. The effective cross section with which backgrounds will be compared is .30 nb. The forward and backward calorimeters will only be used to detect the presence of additional gamma rays in each event. Events with more than 2γ rays will not be used in the η_c analysis. Since we expect that accidentals will eliminate good events 10% of the time, the effective cross section

will be reduced by 10%. The effect of cracks and analysis cuts will reduce the detection efficiency by another 5% and 10% respectively. When all these reductions are included the effective cross section will be reduced to .22 nb.

b) Dominant Background Channel:

While the background consists of states with 2 or more π°'s, the only process which makes a significant contribution to the background is

(5) $$\bar{p}+p\rightarrow\pi^\circ+\pi^\circ$$

A measurement of the differential cross section for (5) in the kinematic region of interest can be obtained from the R-704 data. They find that the integrated value of the cross section in the angular interval corresponding to $|\cos\theta|< .55$ is 58 nb.

This figure must be compared with a cross section of .3 nb for reaction (1) integrated over the same angular range. In order to achieve a signal to noise ratio of at least 1 to 1 the $\pi^\circ\pi^\circ$ background must be suppressed by a factor of 200 relative to the 2γ signal. To be on the safe side we designed the detector so that the probability for incorrectly identifying a π° as a single gamma ray will be 3% or less. This will provide a signal to background ratio of 5 to 1.

A $2\pi^\circ$ event will simulate reaction (1) only if both π°'s from reaction (5) decay asymmetrically and if both low energy, backward emitted photons escape detection. Moreover the measured direction of the forward emitted photons must be consistent with what is expected from the two body

kinematics of reaction (1) within the errors of energy and angular resolution. The calorimeter profile was chosen so that the minimal separation between photon trajectories from reaction (5) at the calorimeter entrance is >11 cm or >2.75 times the transverse dimension of one calorimeter tower. Figure 1 shows the distribution of photon-photon separation at the calorimeter entrance for the π^{o}'s from reaction (5).

We estimated the efficiency for discriminating between reaction (1) and (5) by a Monte Carlo simulation of the proposed detector which contained the following assumptions. The simulation includes the spatial resolution and the energy resolution of the lead glass blocks. We assume that a photon will be detected in the forward calorimeter when its energy exceeds 100 MeV. We assume that all photons emitted at angle smaller than 2° with respect to the p beam will escape detection. In an effort to simulate the effect of cracks we assume that 5% of all other photons will escape detection. We assume that the calorimeter support system, cerenkov mirrors, and track chamber will present $(10/\sin\theta_L)\%$ of radiation length to all photons. The effect of this material is included in the simulation.

Since the ability to discriminate the 2γ final state from $2\pi^{o}$ state depends on the low energy cut off of the central calorimeter and the backward calorimeter we tried several cutoff energies in the simulation. The results are summarized in Table I.

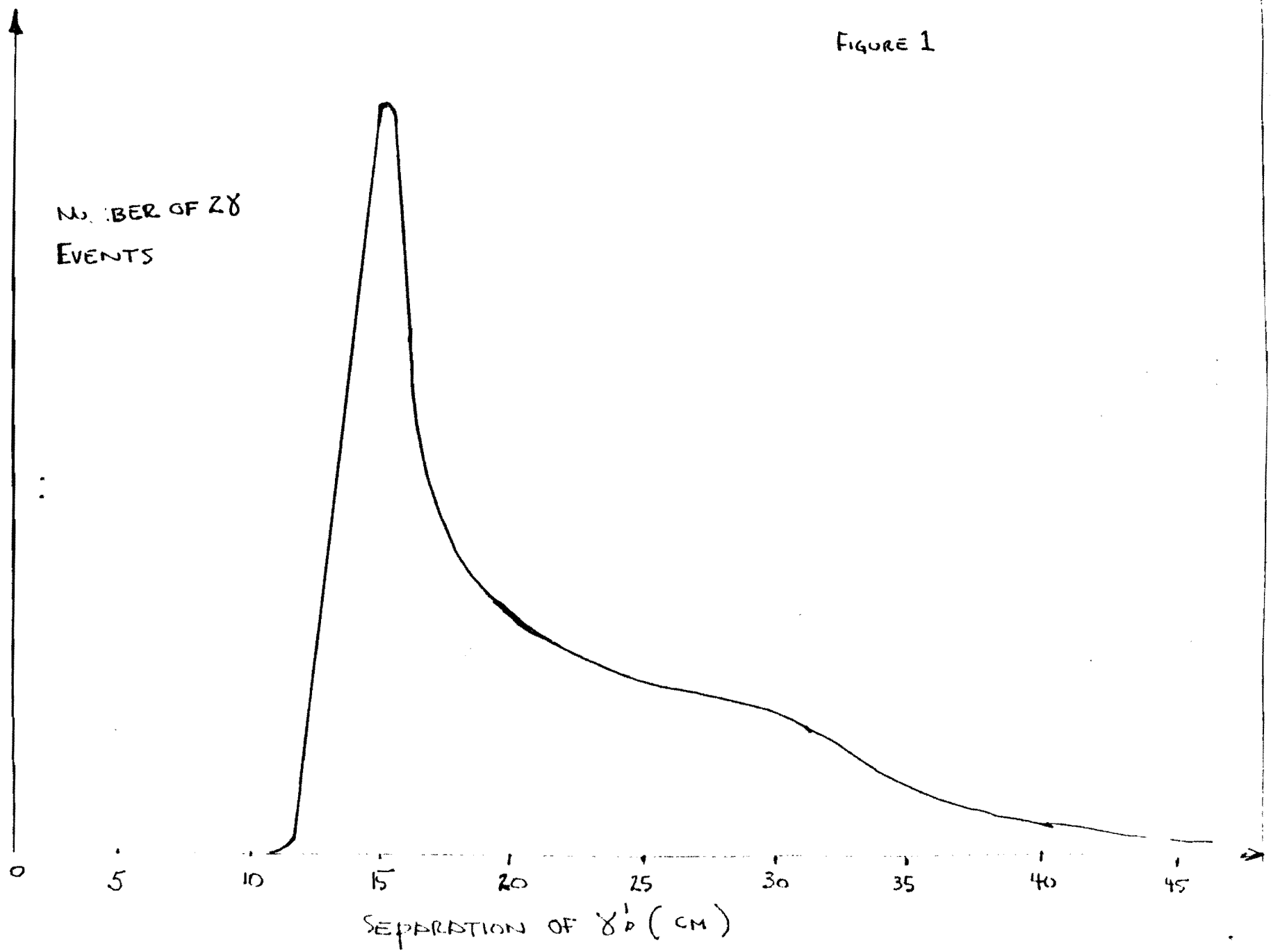
NUMBER OF 2γ
EVENTS
0
5
10
15
20
25
30
35
40
45
SEPARATION OF γ'S (CM)

FIGURE 1

Table I - Results of Monte Carlo Simulation of $\eta_c \to \gamma\gamma$

Central Calorimeter Energy Cut Off	Backward Calorimeter Energy Cut Off	$\pi^\circ\pi^\circ$ rejection Factor
40 MeV	30 MeV	10×10^{-4}
50 MeV	50 MeV	13×10^{-4}
40 MeV	1000 MeV*	16×10^{-4}
100 MeV	100 MeV	47×10^{-4}

*this is equivalent to not detecting backward photons

This Monte Carlo simulation shows that with the proposed segmentation the probability of misidentifying reaction (5) as a 2γ final state is between .1% and .2%, depending on how efficient the backward calorimeter is made.

The only other states which can contribute significantly are $3\pi^\circ$, $\omega^\circ(\pi^\circ\gamma)+\pi^\circ$ and $4\pi^\circ$. We note that the 58 nb cross section for $\pi^\circ\pi^\circ$ production, quoted earlier, is actually the inclusive $\pi^\circ\pi^\circ+x$ cross section when the particles comprising x carry less than 20% of the total energy and escape detection. For that reason the previous estimate includes these other background processes. While the process whereby 2γ's are produced directly in a $\bar{p}p$ collision rather than the decay of a resonant state is also a possible source of background. Since the cross section was at or below the limit of detectability of R704 it should present no problem to P-7601,5).

c) Signal to background

We estimate on the basis of the preceding that the signal to background ratio will approach 3 to 1, which is more than sufficient to extract a signal.

d) Integrated Luminosity Requirements

Since the width of the η_c is about 11 MeV, roughly 30 times the expected resolution, we can measure it very accurately. We plan to measure the cross section for 2γ production to a statistical accuracy of 1 event/pb at ten energies over the whole resonance, including some control points off resonance. Since a yield of 1000 η_c events decaying into 2γ's should be adequate to accurately measure the mass and width, an integrated luminosity of 1.5x1037cm-2 seems appropriate. This will require 400 hours of data taking at a luminosity of 1031 cm-2 sec-1.

2. $^1P_1$ Production

(6) $\bar{p}p \to {}^1P_1 \to \psi + x$

a) Cross Section Estimate

While the PAC asked us to discuss the case where x consists of $2\pi^0$'s, we give here instead a more general discussion of the $^1P_1$ into $\psi+x$. As in reaction (1) we need to estimate the value of the resonance parameters: m_p, Γ_{tot}, $\Gamma(^1P_1 \to \bar{p}p)$ and $BR(^1P_1 \to J/\psi\pi\pi)$.

Theoretical estimates for the mass and total width are:

$$m(^1P_1) \approx \frac{(\Sigma(2J+1)m(^3P_J))}{\Sigma(2J+1)} \approx 3526 \text{ MeV/c}^2 \tag{7}$$

$$\Gamma_{tot}(^1P_1) \sim \Gamma_{tot}(^3P_1) \sim 500 \text{ keV} \tag{8}$$

The partial width $\Gamma(^3P_1 \to p\bar{p})$ has been measured[1] to be 57±18 eV. While we expect $^1P_1$ formation from $\bar{p}p$ to be suppressed relative to $^3P_1$, we are unable to calculate the suppression. Therefore we assume a factor of 4 suppression, leading to an estimate of $\Gamma(^1P_1 \to \bar{p}p) \sim 15$ eV, to be on the safe

side.

An upper limit for the cross section for reaction (6) can be obtained from R704. This limit is conveniently expressed in (9) in terms of the appropriate partial widths.

(9) $\Gamma(^1P_1 \to \bar{p}p) \cdot (\Gamma(^1P_1 \to \psi x)/\Gamma_T(^1P_1)) < 7$ eV

Using this result with the estimate for $\Gamma(^1P_1 \to \bar{p}p)$, the $BR(^1P_1 \to \psi + x)$ should be less than 50%.

While we are unable to obtain a reliable estimate of the branching ratio into $J/\psi\pi\pi$, we make three observations which lend support to the proposition that $BR(^1P_1 \to \psi + x)$ is large. First, the decay $\psi' \to \psi\pi\pi$ is the dominant channel with a branching ratio of 50%. The large partial width can be understood in QCD based theoretical models[6]. While these calculations cannot be easily extended to the $^1P_1$ case since the approximation used fails when the phase space is very small, one expects that only channels containing charmonium have partial widths as large as 100 keV. Second, the the only other allowed state with appreciable phase space is the radiative decay

(10) $^1P_1 \to \eta_c + \gamma$

As in the case of the $\chi_1(^3P_1)$ and ψ', and ψ the $^1P_1$ annihilation channels must proceed through three gluons and the total width for decay into three gluon is expected to be of the order of 50 keV. Third, the alternative decay mode of $^1P_1 \to \eta_c\pi\pi$ is forbidden by C conservation. For the purpose of estimating the cross section we assumed that $BR(^1P_1 \to \psi + x)$ is 10% and Γ is 500 keV. Using (7) and (8) we estimate the cross section for

detecting the J/ψ's through its decay into e^+e^- at the $^1P_1$ at the resonance peak to be

$$(11) \qquad \sigma(m_R)=(3\pi(\bar{h}c)^2/P_{cm}^2)((\Gamma(^1P_1\to\bar{p}p)/\Gamma_{tot})\ BR(^1P_1\to J/\psi+x) = 4.8\ nb$$

Since the ψ is detected through its e^+e^- decay mode the effective cross section of interest is reduced by .074 to 355 pb.

A Monte Carlo simulation of the proposed detector shows that geometric efficiency for detecting the e^+e^- pair from the ψ simultaneously in the central calorimeter and the cerenkov counter is 54%. When the geometric efficiency to detect the e^+e^- pair is included the effective cross section is reduced to 200 pb. We reduce the effective cross section by an additional 25% in order to include the events which will be lost to the cerenkov counter inefficiency, cracks and analysis inefficiency. Thus the effective cross section is 150 pb. In closing this section we note that we should be able to see the $^1P_1$ provided the unknown branching ratio is > 1%.

b) Background Estimate

There are two sources of background. The first and most significant comes from (12) when the "h^+h^-" pair is misidentified as an e^+e^- pair and its mass is equal to 3.1 GeV/c^2 within experimental errors. In most cases the h^+h^- is a pair of charged hadrons such as pp, $\pi^+\pi^-$ or K^+K^-. In some instances however $h^\pm$ can be a γ which converts in the beam pipe and thus leaves a track in the track chamber and counts in the calorimeter.

$$(12)\ p+p \to \text{"}h^+h^-\text{"} + x$$

The second occurs when a ψ is produced inclusively without proceeding through a resonance.

(13) $\bar{p}+p\rightarrow\psi+x \qquad (x=\pi^\circ,\ \pi^+\pi^-,\ \pi^\circ\pi^\circ,\ldots)$

While (12) is truly background (13) is interesting in its own right. As will be discussed later, the cross section for inclusive ψ production is small compared to our estimate of the cross section for reaction(6).

The specific channels in (12) which can make major contributions to background are h^+h^-, $h^+h^-\pi^\circ$, $h^+h^-\pi^\circ\pi^\circ$, and $h^+h^-\pi^+\pi^-$. h^+h^- pairs are distinguished from e^+e^- pairs by the cerenkov counter and energy deposition in the shower counter. The h^+h^- system must have 80% or more of the total energy if it is to pass the calorimeter cuts. Since the details of construction of the proposed P-760 detector will be different from the R-704 detector, it is worth reviewing the way a false electron signal can be generated.

An electron signature can be simulated by two types of events: delta rays and e^+e^- pairs from either internal or external conversion. A charged pion produces a signal in the cerenkov counter when it creates a δ ray with an energy of 20 MeV or more in the cerenkov radiator. In order for the π to be misidentified as an electron it must also charge exchange in the calorimeter giving rise to an electromagnetic shower with the full energy of the π. A Dalitz decay or the conversion of a photon in the vacuum chamber wall or track chamber will give a signal in the cerenkov and an electromagnetic shower in the calorimeter.

The contribution from delta rays can be suppressed by minimizing the

amount of material that the pions traverse. It was established in R-704 that the charged pion misidentification can be reduced by the cerenkov requirement alone, to the 10^{-3} level[1].

The contribution from pair conversions in the beam pipe will be small. By using a thin wall (1 mm) Beryllium pipe segment, around and downstream of the interaction point this component can be kept at or below the level of Dalitz decays (1.2%). Even when the electron and positron tracks are unresolved by the tracking chambers, this background can be reduced further by requiring that dE/dx in the track chamber (>6 samplings in the track chamber) and cerenkov signal amplitude be compatible with one electron. These requirements will improve the electron identification with respect to R-704.

Finally, the requirement that the two electron candidates reconstruct as an e^+e^- pair with the mass of 3 GeV/c^2 will reduce the background by another factor of 10^3 to 10^4.

In Table II we summarize the differences in the two detectors that are relevant to the present discussion.

Table II

		P760	R704
Acceptance	$\Delta\phi$	$\sim 2\pi$	$\sim \pi/2$
	$\Theta_{min}-\Theta_{max}$	17°-60°	18°-66°
	ε	54%	11%
Cerenkov	α_{min}*	$\lesssim 17°$	$\gtrsim 28°$
	$\langle n \rangle$	5	5
dE/dx	detector	track chamber	scintillator
	# samplings	6-9	1
Radiation length	17°	10^{-2}	5×10^{-2}
before tracking	41°	4.3×10^{-3}	2.8×10^{-3}
	60°	3.3×10^{-3}	4×10^{-2}
Calorimeter	long. segm.	none	yes: $4.7\chi_0$; $10\chi_0$
	σ/E	$.05/\sqrt{E}+.02$	$.12/\sqrt{E}+.02$

*α_{min} is the angle below which the pion from $p\bar{p}\to\pi\pi$ is above threshold in the cerenkov.

P-760 is better than R-704 in all aspects except one; the calorimeter is not segmented longitudinally. To understand how the lack of longitudinal segmentation effects the background we have deleted all requirements on the longitudinal development of the shower in an analysis of the R-704 data. No new event is accepted in the J/ψ mass region ($m_{e^+e^-}>2.6$ GeV) when these requirements are deleted. Given the shape of the background shown in Figure 2 we estimate that the better energy resolution of P-760 will improve the background rejection

Rather than resort to a complete Monte Carlo simulation we have again made use of the findings of Ref. 1 to give quantitative estimates of the residual background to the J/ψ inclusive production channel. In an energy scan in the region $3520<\sqrt{s}<3531$ MeV/c² an integrated luminosity of 1017^{-1}nb was devoted to the study of $J/\psi+x$ final states. One analysis chain, which preserved ~70% of the signal, required that the electron candidates pass a set of cuts designed to suppress backgrounds from delta rays and e^+e^- pairs. Figure 2 shows the mass distribution of events which did not pass the cuts, but which satisfied the cerenkov trigger. Since all cuts were independent of the final e^+e^- mass value, one could estimate from the residual background in the low mass region ($2200<m_{e^+e^-}<2600$ MeV/c²), the residual background under the $m(J/\psi)$ mass peak. The limit corresponds to 1 event (90% C.L.) per pb cross section in the (~10%) acceptance. With the full azimuthal coverage of P-760 the geometrical acceptance, the cross section limit will increase by a factor of ~5 to 5 pb.

The aforementioned results also limit the cross section for continuum production of $\psi+x$. A theoretical estimate of the process $\bar{p}+p\rightarrow\psi+\pi^\circ$ has been made and the cross section at $m_{\bar{p}p}=3526$ MeV/c² is 220 pb. When the

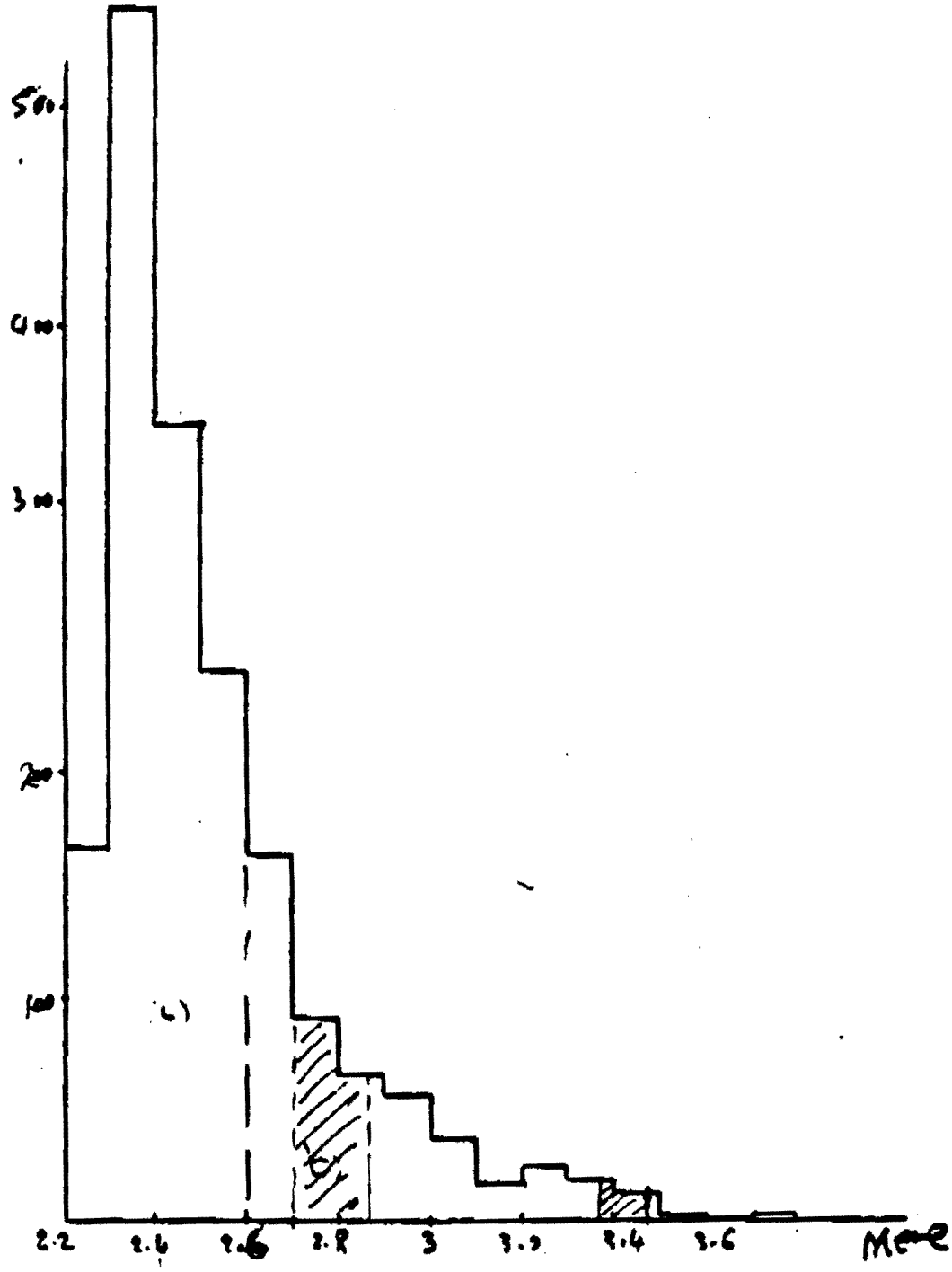

Figure 2

e^+e^- Invariant mass spectrum of events which do not survive the last selection

branching ratio for the ψ decaying to e^+e^- and the 50% geometric efficiency for detecting the e^+e^- and π° is considered the effective cross section is 9 pb. This is compatible with the sensitivity of R-704. The production cross sections for other non-resonant states such as $\psi\pi^+\pi^-$ are expected to be comparable or smaller.

c) Estimated Signal to Background Ratio

The estimated signal to background rates for the processes discussed in b) is 10 to 1. While this may be an overestimate because of the uncertainty in BR($^1P_1 \rightarrow \psi x$), the signal to background will be 1 to 1 as long as the branching ratio is greater than 1%.

d) Predicted rates

We proposed to run for 200 hours at the resonance peak, assuming the location of the resonance is established quickly, and a comparable amount of time away from the resonance. At a luminosity of 1031 cm-2 sec-1 this will result in an integrated luminosity of 1.5x1037 cm-2. Such an integrated luminosity will provide the following yields:

$p\bar{p} \rightarrow {}^1P_1 \rightarrow \psi + x$	750 events on resonance
$p\bar{p} \rightarrow \psi + \pi^\circ$	130 events off resonance
$p\bar{p} \rightarrow h^+h^- + x$	75 events or less are misidentified as $\psi + x$.

It should be noted that the geometric efficiency for detecting x when x is $\pi^+\pi^-$ or $\pi^\circ\pi^\circ$ is in excess of 80%. For that reason it should be possible to distinguish among the cases where x is a π°, $\pi^+\pi^-$, and $\pi^\circ\pi^\circ\pi^\circ$ when the sample of $^1P_1$ decays has 750 events. The detector has been designed with tracking capability over essentially all the solid angle occupied by the π^+, π^- tracks ($\theta<60^\circ$). We estimate that 20% of the signal will be lost either because the π goes forward at every small angle or because it hits a cerenkov phototube assembly. The measurement of the two π directions will allow us to fully reconstruct the event, providing a very clean signature.

As for the $2\pi^\circ$ final state, which the PAC specifically requested, its identification is based on the detection of $>3\gamma$ from the π° decays. The detection efficiency has been calculated by Monte Carlo simulation. After introducing appropriate energy cuts in the simulation of (see discussion on $\eta_c\to\gamma\gamma$) the calorimeter elements we find the acceptance to detect the $2\pi^\circ$'s to be ~85%.

It should be possible to analyze the various final states if the number of events is as large as 750 events. Table III summaries the kinematically allowed decays.

Table III. Allowed Final States for $^1P_1 \to J/\psi + x$

State	Isospin	Angular* Momentum	Comment
π°	1	0	Isospin forbidden, 2nd order electromagnetic
$(2\pi)^0$	0	1	Isospin allowed
$(3\pi)^0$	1	0	Isospin forbidden, 2nd order electromagnetic

*Relative angular momentum of ψ and x

The decays $J/\psi + x$, $J/\psi + 2\pi((I=1)$, $J/\psi + 3\pi/(I=0)$ are all forbidden by charge conjugation, since x must be 1^{--} (or 3^{--}, 5^{--},....). Since the probability of there being anything other than a π° or a 2π state is very small, the identification of the various final states should be straightforward.

We note that the I-spin violating transition $^1P_1 \to J/\psi + \pi^\circ$ could have a rate larger than expected. A significant non-resonant component is also expected in this final state channel (~20 pb cross section in the $e^+e^-\gamma\gamma$ final state). The probability to detect both photons in the calorimeter is >90%. Again because the event can be completely reconstructed, the signal should have very little background.

Summary of the Request for Running Time

It seems appropriate to summarize our initial request for data taking here. The requirement for the $^1P_1$ and η_c is 800 hours. In addition we will request 400 hours of running at the J/ψ, χ_1, χ_2, and ψ'. The J/ψ is needed to calibrate the machine energy. We also want to spend 400 hours to

determine if the η_c' can be detected and to search the D region for narrow states which may be forbidden from decaying into charmed mesons. Should these measurements show that the mass and width of these states are measurable by this technique we would plan to make an additional request for running time. Prior to the start of taking data we will need at least 800 hours to make the Accumulator work in the fixed target variable energy mode. We would also like to carry out an initial energy scan to determine the energy range over which the Accumulator will work. In particular we would like to establish the lowest possible operational energy. In particular, we would like to determine if operation at 1622 MeV/c antiproton momentum, corresponding to $\sqrt{s}$=2.2 GeV is feasible. It should be noted that the running time requested refers to the time during which 15 milliamps are circulating in Accumulator at the energy of interest. It does not include filling time. We estimate that filling time will represent one third to one quarter of the total operating hours. Thus, this request corresponds to a scheduled period of 30 weeks at 100 hours/week. It is hoped that the machine development and background studies can be carried out early in 1987 and that the physics run can start late in 1987.